

UC Berkeley

SEMM Reports Series

Title

Finite Element Analysis of Tubular Joints

Permalink

<https://escholarship.org/uc/item/61n8r6n8>

Authors

Greste, Ojars

Clough, Ray

Publication Date

1967-04-01

LOAN COPY

Please return to:

NISEE/COMPUTER APPLICATIONS
TANEN HALL
UNIVERSITY OF CALIFORNIA
BERKELEY, CALIFORNIA 94720
(415) 842-5113

REPORT NO.
67-7

STRUCTURES AND MATERIALS
DEPARTMENT OF CIVIL ENGINEERING

FINITE ELEMENT ANALYSIS OF TUBULAR JOINTS: A REPORT ON A FEASIBILITY STUDY

By
OJARS GRESTE
and
RAY W. CLOUGH

Report to the Sponsors: Standard Oil Company
of California, San Francisco, California

APRIL 1967

STRUCTURAL ENGINEERING LABORATORY
COLLEGE OF ENGINEERING
UNIVERSITY OF CALIFORNIA
BERKELEY CALIFORNIA

Structures and Materials Research

Department of Civil Engineering

Report No. 67-7

FINITE ELEMENT ANALYSIS OF TUBULAR JOINTS

A Report on a Feasibility Study

by

Ojars Greste

and

Ray W. Clough

Submitted to

Standard Oil Company of California

University of California

Berkeley, California

April 1967

TABLE OF CONTENTS

	Page
PREFACE	ii
INTRODUCTION	1
Background	1
Purpose and Scope	2
METHOD OF ANALYSIS	2
Finite Element Method	2
Cylindrical Shell Analysis	5
SCHEDULE OF ANALYSES	6
Preliminary Investigations	6
Cases Studied	7
RESULTS OF ANALYSIS	12
Comparison with Case S	12
Comparison of Line Load and Branch Cases	13
Comparison with Experimental Results of Toprac	15
Results for Y and K Joints	16
CONCLUSION	16
REFERENCES	17
LIST OF FIGURES	20

PREFACE

This investigation was carried out under a research contract with the Standard Oil Company of California. The computer analyses were performed by Mr. Ojars Greste, graduate student, under the direct supervision of Professor Ray W. Clough, Department of Civil Engineering. The general shell analysis computer program which was used in the investigation was developed by Mr. C. P. Johnston, graduate student, in his Ph.D. dissertation research. All computer analyses were carried out on the IBM 7094 computer operated by the University of California Computer Center. Mr. P. Sharifi assisted with preparation of data for some of the analyses.

INTRODUCTION

Background

In recent years, increasing interest has been shown in the performance of joints in framed structures fabricated from tubular sections, particularly as a result of the oil industry's use of such members in the construction of off-shore drilling platforms. Several failures of these structures have prompted an evaluation of existing design methods, and have led to a number of experimental and analytical investigations into the behavior of welded connections between tubular sections (1-5)*.

The stress analysis of the joints between tubular members constitutes an extremely complex problem in mechanics, involving the intersection of two cylindrical shell surfaces. Standard methods of shell analysis can deal with the problem only approximately, because of the awkward boundary conditions presented by the intersection line; thus it appears probable that satisfactory solutions can be obtained only by numerical procedures applied by means of digital computers. This report describes the results of a feasibility study concerning the effectiveness of one such numerical procedure, the finite element method, in the analysis of tubular joints.

* Numbers in parentheses designate References listed at the end of the report

Purpose and Scope

The purpose of this investigation was to determine the accuracy and reliability of an existing finite element shell analysis program in the evaluation of stresses and deflections in typical tubular joints. The quality of the finite element solutions was established by comparison of its results with those obtained by another analytical procedure (a cylindrical shell program) as well as with one set of experimental results obtained by Toprac at the University of Texas⁽⁴⁾.

Six different joint geometries were considered in these studies: four concerned a simple Tee-joint as shown in Fig. 1b; the others were a Y-joint and a K-joint as shown in Figs. 1c and 1d. In all cases the loads were applied axially through the bracing members, as indicated in the figures. For three of the Tee-joints two solutions were obtained for each configuration, the first employing a prescribed line load on the main member to represent the effect of the branch member, (Fig. 1a), the second including a short section of the branch member (Fig. 1b).

METHOD OF ANALYSIS

Finite Element Method

The finite element method of analysis used in this study is an extension of a technique which was first applied to the solution of plane stress problems⁽⁶⁾. In subsequent developments, the method was adapted to the analysis of axi-symmetric solids⁽⁷⁾ and plate-bending problems⁽⁸⁾, of axi-symmetric shells⁽⁹⁾, and of thin shells of

arbitrary geometry⁽¹⁰⁾. The computer program which was used in this investigation is an improved version of the general thin shell analysis program, and has been described in a previous publication⁽¹¹⁾; only a brief outline of the method will be presented here.

The basic concept of the finite element procedure is the idealization of the actual continuum as an assemblage of discrete structural elements. In the present shell analysis program, the arbitrary shell surface is approximated by a system of triangular flat plate elements, the corner (or nodal) points of which lie on the mid-surface of the actual smoothly curved shell. The solution requires first the evaluation of the stiffness properties of the individual elements; the stiffness properties of the complete assemblage are then derived by superposition of the element stiffnesses. Finally, the analysis of the shell is accomplished by simultaneous solution of the discrete nodal point equilibrium equations for the nodal displacements.

It is important to note that the finite element idealization of the shell introduces two forms of approximation into the analysis. First, the set of flat triangular plate "facets" provides only an approximation to the smoothly curved surface of the actual shell. Thus the shell which is analyzed differs slightly from the actual shell. Second, the stiffness properties of the individual elements are derived on the basis of an assumed set of displacement patterns within the elements; thus constraints are imposed on the manner of deformation of the shell. However, the errors associated with both types of approximation tend to diminish with reduced mesh sizes in the finite element idealization, and the results of the examples presented in this report demonstrate that excellent solutions can be obtained with reasonable mesh refinements.

The most critical step in the finite element analysis is the evaluation of the stiffness properties of the individual elements. It is assumed that the elements are interconnected only at their corner points, thus the element stiffness represents the forces at these nodal points resulting from unit displacement of the nodal points. Two types of element stiffness are considered in the shell analysis: membrane stiffness which relates forces and displacements in the plane of the elements, and plate bending stiffness which takes account of displacements and rotations out of the element plane. Because the element is a flat plate, there is no coupling between these types of element stiffness properties; therefore it was possible to use a standard plane stress element to represent the membrane stiffness of the shell⁽⁶⁾, and a standard plate bending element to represent its flexural stiffness⁽⁸⁾.

The plane stress membrane element has two degrees of freedom at each corner -- two components of translation in the plane of the element, while the plate bending element has three degrees of freedom at each corner -- translation normal to the plane and rotation about two axes in the plane. Thus when these elements are assembled into the shell idealization they provide only five degrees of freedom at each joint; the rotation about the axis normal to the shell surface is assumed to be zero. In the case of a smoothly curving shell, the constraint implied by this assumption is not severe -- rotations of this type can be expected to be small in comparison with the other displacement components. At the intersection of two shell surfaces such as in a tubular joint, however, this constraint in two different planes requires that rotations take place only about the intersection

line of the two planes. This possibly might constitute a serious deficiency in the present form of the finite element analysis procedure. Elimination of this constraint by the introduction of the additional rotational degree of freedom in each element was beyond the scope of the present study. However, such modification of the method is possible and this factor will be investigated in a subsequent study.

Cylindrical Shell Analysis

In order to evaluate the effectiveness of the finite element analysis procedure, it was necessary to obtain numerical results by another procedure for comparison. The most reliable analytical tool available to the investigators was a digital computer program for the analysis of cylindrical shells which had been developed at the University of California by Professor A. C. Scordelis⁽¹²⁾. This computer procedure is based on the Donnell cylindrical shell equations. The system considered and the five types of loading that can be treated are shown in Fig. 2. The circular tube (subsequently referred to as the chord) is simply supported at each end by a diaphragm rigid in its own plane, but of zero stiffness normal to that plane. Each load is defined by its total magnitude, uniformly distributed length (δ), and location on the tube (ξ, φ). The moments M_x and M_z are approximated by radial and tangential loads respectively, distributed in such a way as to be statically equivalent to the moments. Loads may be input in any combination along one or more generators of the tube and may differ for each generator.

In the Tee-joint analysis, it was assumed that the branch tube

is infinitely rigid in its longitudinal direction as compared with the radial flexibility of the chord wall. This implies that a uniform vertical displacement was applied to all points on the tube intersection. In addition it was assumed that rotations and horizontal deflections at the intersection line were unrestricted.

The analysis was carried out by dividing the tube intersection line into a number of short segments, applying unit loads to each segment, and calculating the resulting deflections by means of the Scordelis program. This set of flexibility coefficients was then inverted to obtain the stiffness coefficients of the load points on the joint intersection line. With these coefficients, it was possible to determine the forces required at each load point to produce the desired uniform displacement condition at the joint. Finally, the chord member was analyzed by the Scordelis program for the stresses and deflections produced by this prescribed load condition. The results of the analyses carried out by the Scordelis program in this study are referred to hereafter as Case S.

SCHEDULE OF ANALYSES

Preliminary Investigations

Before commencing the analyses for the six afore-mentioned configurations, a number of exploratory studies were carried out for the Tee-joint (Figs. 1a and 1b). The results of these studies were reported in Reference 13 and are only briefly summarized here.

The geometry of the system of Fig. 1a (referred to herein as the line load case) was defined by the ratios $d/D = 0.6$, $t/D = 0.01$, and

$L/d = 5$, which were chosen to correspond with a case previously studied by Professor Scordelis. Finite element analyses of this system were performed using two different types of loadings: (1) uniform vertical displacements applied at all nodal points, around the line of intersection, and (2) vertical forces applied at all nodal points of the intersection line and distributed as computed in Case S for a uniform applied displacement. For the Case S the two types of loading are, of course, equivalent. However, for the finite element case, because of the constraints imposed on the shell deformation by assuming certain modes of displacement within each element, the idealized structure is somewhat stiffer than the real structure. The two analyses were performed in order to ascertain whether the two conditions of loading would produce equivalent results in the finite element case. Four different finite element idealizations, ranging from a coarse to a fine mesh, were employed in the analyses.

The results showed that:

- (i) Refinement of the mesh caused successive finite element solutions to converge toward the Case S solution, and
- (ii) for the finest mesh idealization, the line displacement input and the force input cases were equivalent.

In addition to the line load cases, several analyses were carried out for the system shown in Fig. 1b in which the branch member was considered. The d/D , t/D , and L/d parameters for this structure were the same as those for the line load case. The only additional parameter required to define the branch case was the branch length-to-diameter ratio, for which the values 1.0, 1.5, and 2.0 were considered. The loading consisted of either uniformly imposed displacements or

uniformly distributed forces applied at the end of the branch.

The results of these analyses demonstrated that the length of the branch tube had little direct effect on the stresses and displacements developed in the main member. An indirect effect may be noted in all cases where uniform displacements were applied at the end of the branch member. Due to the axial flexibility of the member the displacements actually developed at the intersection line were smaller than the input deflections, with the amount of this discrepancy depending on the length of the branch member. Making allowance for this effect it was found that the local stresses developed in the main tube were essentially independent of the branch length.

A study also was made to determine whether the type of loading applied to the branch was important. For a branch length/diameter ratio of 2.0, a uniformly distributed force P , and subsequently a uniform displacement which developed the same resultant force, were applied. From these results it was concluded that if the length of the branch was at least twice its diameter, then stresses and displacements developed in the chord member depended only on the resultant force and not its distribution at the end of the branch.

Cases Studied

The configurations of the joint types studied are shown in Fig. 1. A total of six different geometries were considered: four Tee-joints (designated T-1, T-2, T-3, T-4) and one each Y joint and K joint. In each case the chord tube was simply supported and had a rigid diaphragm at each end. The dimensions of joint T-2 were chosen to correspond with a case studied experimentally by Toprac and others⁽⁴⁾, while

those of T-1, T-3, and T-4 were chosen to correspond with cases studied analytically by Professor Scordelis.

For each of joints T-1, T-3 and T-4 two loading cases were considered: a line load case in which the branch was omitted; and a branch case in which the presence of the branch was considered. The former of these was the case actually compared with the Case S results and the load input consisted of a uniform vertical displacement applied at all nodal points around the line of intersection. For the branch case the input was a force, equivalent to that developed in the line load case displacement, uniformly distributed around the end of the branch member (although as noted above the manner of distribution is not critical).

For the Y and K joints no quantitative comparisons were made. For the K joint the force in the inclined branch member was such that its vertical component balanced the force in the other branch member. The horizontal force component was distributed uniformly around the left end of the chord tube wall, and a point at mid-depth of the tube was fixed against horizontal displacement. In the case of the Y joint the same loading was considered except for the absence of the vertically applied force.

The dimensions, elastic properties, and applied loadings used for all joints are listed in Table I. With the exception of joint T-2, the length measurements and the force quantities are expressed in terms of an arbitrary system of units, following the procedure adopted by Professor Scordelis.

TABLE I: PROPERTIES OF TEST JOINTS

<u>Property</u>		<u>T-1</u>	<u>T-2</u>	<u>T-3</u>	<u>T-4</u>	<u>Y</u>	<u>K</u>
Chord Diam:	D	1.0	12.50 inch	1.0	1.0	1.0	1.0
Chord Length:	L	2.7	48 inch	3.5	3.5	2.8	2.8
Branch Diam:	d	0.3	2.672 inch	0.7	0.7	0.3	0.3
Chord Thick:	t	0.01	0.250 inch	0.01	0.02	0.01	0.01
Branch Thick:	t_b	0.01	0.203 inch	0.01	0.01	0.01	0.01
Young's Mod:	E	10^6	30,000 ksi	10^6	10^6	10^6	10^6
Poisson Ratio		.3	0.3	0.3	0.3	0.3	0.3
Applied force	P	1000	1.70405 kips	1000	1000	1000	1000
Applied displacement		4.1757	---	1.7796	0.5409	---	---

Note: Except for Joint T-2, all properties are expressed in arbitrary length and force units

The finite element idealizations for the chord and branch tubes, in the form of their developed surfaces, are shown in Figs. 3 and 4. Because of symmetry properties, only one quarter of each Tee-joint and one half of each of the Y and K joints was considered. The same basic mesh layout scheme was used for all four Tee-joints (Fig. 3a) with local modifications to allow for the differences in the chord lengths and branch diameters. Figs. 3b and 3c show the layout modifications in the pipe intersection region for joints T-1 and T-2. The scale of T-2 in Fig. 3c in relation to the other Tee-joints is such that the chord diameters are all equal. The layout for the branch, shown in Fig. 3a is typical for all the Tee-joints.

The computer solution utilizes the property that the stiffness matrix of the finite element assemblage is banded and a limitation is imposed on the size of the half band width. The half band width depends on the node numbering scheme used and governs the degree of mesh refinement possible in the pipe intersection region. To obtain the half band width the entire array of elements is scanned and the maximum difference between the numbers of any two nodes associated with a particular triangle is recorded. The half band width is then given by one plus this number multiplied by five. In the computer program the maximum available half band width was 100; that is, the difference in node numbers for two adjacent nodes cannot exceed 19. The mesh layouts shown in Figs. 3 and 4 give the maximum refinement possible in the pipe juncture region with the permissible half band width.

In addition to the above restriction, the maximum number of nodes and elements are limited in this program to 540 and 980 respectively. The number of nodes and elements for each of the cases studied here are summarized in Table II.

TABLE II: DIMENSIONS OF THE FINITE ELEMENT IDEALIZATIONS

<u>Joint</u>	<u>Number of Nodes</u>	<u>Number of Elements</u>
T-1	413	734
T-2	474	846
T-3, T-4	416	740
Y	438	753
K	538	973

RESULTS OF ANALYSES

Comparison with Case S

An explanation of the notation used for presenting the results is shown in Fig. 5. Figures 6 through 12 show comparisons of results obtained by the finite element analyses with those of Case S. Radial and tangential displacements at the center section of the chord tube are shown for joint T-1 in Fig. 6 and for joints T-3 and T-4 in Figs. 7 and 8. In addition, vertical displacements along the top and bottom of the chord tube are plotted for joint T-1 in Fig. 6. The comparison is seen to be very favorable: the displacement quantities of Case S are matched almost exactly by the finite element results.

Values of circumferential and longitudinal moments are shown in Figs. 9 and 10. The finite element results again closely approximate the Case S results and differ noticeably only in the region of moment concentration where the line load is applied. For joint T-1 the peak circumferential moment M_x differs from Case S by 7%. The corresponding figures for joints T-3 and T-4 are 18.7% and 16.5% respectively. The preliminary studies showed that a fine finite element mesh was required in the critically stressed region to reproduce the high moment gradients predicted by Case S. The results presented here utilized the greatest mesh refinement possible for the present computer program capacity. Refinement of the mesh shown in Fig. 3 for this critical area should lead to further improvement of the finite element results.

The finite element membrane forces are compared with Case S results in Figs. 11 and 12. Although the overall agreement between

the two cases is not as good as for the moment quantities, the distribution of the forces across the sections in question is adequately represented. The membrane forces at each nodal point were obtained in the finite element analysis by taking the arithmetic mean of the appropriate values for all the elements having that nodal point in common. The element properties are such that the membrane forces are constant throughout each element and so in a varying stress field there exist stress discontinuities between elements. Because of this, the arithmetic mean of the stress values surrounding a nodal point may not give the best representation of stress at that point. Studies by others at the University of California, Berkeley, indicate that in regions of high stress gradient a better stress representation may be obtained by a weighted averaging procedure. It is intended to explore this idea in a later investigation.

Comparison of Line Load and Branch Cases

No quantitative results were available for comparison with the branch case analyses. The results are evaluated qualitatively here by comparison with the line load case analyses. Displacement results for joints T-1, T-3 and T-4 are presented in Figs. 13, 14 and 15. For joint T-1 the branch case displacements are everywhere smaller than those for the line load case. This is in accord with the qualitative reasoning that the presence of the branch increases the overall stiffness of the structure, with a significant local effect in the tube juncture region. Joint T-3 behaves in a similar manner generally but with some difference at the crown of the chord tube. Here, because of the restraint offered by the branch to rotation of the chord tube

wall, the branch case radial displacement is actually greater than the line load case displacement. In the case of joint T-4, however, contrary to the above discussed behavior, the branch case displacements are greater than those for the line load case. This is unexpected and no satisfactory explanation can be offered at this time.

Moments and membrane forces are shown in Figs. 16 to 19. In all cases the peak values, in the vicinity of the tube intersection, are found to be reduced in the branch case. This is in agreement with the concept of the branch serving as a local force re-distributing element. It should be noted that in joint T-4 the force quantities in the branch case differ from the line load case in a manner consistent with that observed in joints T-1 and T-3. This fact makes more puzzling the discrepancy in displacements observed in Figs. 14b and 15b.

Surface stresses around the circumference and along the top of the chord tube are shown for each joint in Figs. 20 and 21. Of note here is the difference between the peak stresses of joints T-1 and T-3 and between those of joints T-3 and T-4. In the former case the difference is due primarily to the change in the d/D ratio; in the latter case the decrease in peak stresses of joint T-4 is due to the greater chord wall thickness of that joint. In Fig. 22 are shown values of the principal stresses in the outer surface of the chord member at the nodal points on the tube intersection line. The stress magnitudes result from a combination of membrane stress and plate bending, and are plotted radially from the branch tube wall. From Fig. 22a it is seen that the concentration of stress occurs at the point lying on the center section. With an increase in the d/D ratio

there is a reduction of the principal stress magnitudes and a tendency to a more uniform distribution around the intersection line. A similar observation has been made experimentally by Toprac and Brown⁽⁵⁾. Figs. 22b and 22c show the stress reducing effect of increased chord wall thickness in joint T-4.

Comparison with Experimental Results of Toprac

Figs. 23 and 24 show a comparison between surface stresses derived by the finite element analysis of joint T-2 and those obtained experimentally by Toprac and others⁽⁴⁾. The finite element results are somewhat on the low side but the comparison is not unfavorable. Figs. 23a and 24b also show analytical curves obtained by Toprac and others⁽⁴⁾. These were based on the thin shell analyses procedure of Bijlaard⁽¹⁴⁾ in which the axially loaded branch was simulated by a uniformly distributed, radially directed load applied over a square region of the chord wall. On the basis of experimental data, Toprac⁽⁴⁾ modified this theoretical procedure empirically to give better correlation between theory and experiment, but the curves shown in Figs. 23a and 24b are the unmodified results. The finite element results certainly appear good in this comparison.

Fig. 25 shows a plot of vertical displacements along the top and bottom of the chord tube obtained by the finite element analysis together with an experimental result reported in Reference 4. The same reference also reports the measured deflection at the bottom of the pipe. However, this value is greater than the finite element result by a factor of approximately three and so is not plotted on the figure. The results of Fig. 25 do not suggest any firm conclusions.

Results for Y and K Joints

Some of the results from the finite element analyses of the Y and K joints are presented in Figs. 26 to 28. Fig. 26 shows vertical displacements along the top and bottom of the chord tube, Fig. 27 shows surface stresses along the top, and in Fig. 28 are plotted the distributions of principal stresses around the pipe intersection lines. The magnitudes are plotted radially from the branch tube wall. No analytical or experimental comparisons are available for these two joints, thus the results are presented primarily to demonstrate the capability of the finite element method in treating joints of this complexity.

CONCLUSIONS

The results obtained in this investigation demonstrate clearly the potential capability of the finite element method in the analysis of tubular joints. The line load analyses of the Tee-joint systems show that results can be obtained for simple cylindrical structures which agree well with results of an analytical procedure designed specifically for this class of structure and having only limited applicability in tubular joint studies. With the finite element procedure it was possible to study the influence of the branch member in the behavior of the Tee-joint, and thus to evaluate the reliability of the Scordelis analysis for this case.

The comparison with Toprac's work demonstrates that experimentally verifiable results can be obtained by the finite element procedure, while the Y and K joint analyses show the range of configurations which can be treated.

In evaluating the results of this feasibility study, it should be remembered that the finite element computer program which was used was developed originally for the analysis of shell roof structures. Only minor modifications were incorporated into it to accommodate the special characteristics of tubular joints. Several improvements could be made in the program, including the use of refined plane stress elements to obtain a better approximation of the membrane stress distribution, and the addition of the sixth degree of freedom at each joint. With such modifications in the program, and making use of modern computers having greater storage capacity, the potential capability of the finite element method in the analysis of tubular joints appears very great indeed.

REFERENCES

1. Bouwkamp, J. G., "Concept of Tubular-Joint Design", Journal of the Structural Division, Proc. A.S.C.E., Vol. 90, No. ST2, April 1964.
2. Bouwkamp, J. G., "Considerations in the Design of Large-Size Welded Tubular Truss Joints", Engineering Journal, American Institute of Steel Construction, Vol. 2, No. 3, July 1965.
3. Bouwkamp, J. G., "Tubular Joints Under Static and Alternating Loads", Structures and Materials Research, Department of Civil Engineering, University of California, Berkeley, Report No. 66-15, June 1966.

4. Toprac, A. A., Noel, J. S., and Beale, L. A., "An Investigation of Stresses in Welded T-Joints", Structures Fatigue Research Laboratory, Department of Civil Engineering, University of Texas, Austin, Texas, Report Number S.F.R.L. Tech. Rpt. P550-3, March 1965.
5. Toprac, A. A. and Brown, R. C., "An Experimental Investigation of Tubular T-Joints", Structures Fatigue Research Laboratory, Department of Civil Engineering, University of Texas, Austin, Texas, Report Number S.F.R.L. Tech. Rpt. P550-8, January 1966.
6. Turner, M. N., Clough, R. W., Martin, H. C., and Topp, L. J., "Stiffness and Deflection Analysis of Complex Structures", Journal of Aeron. Sci., Vol. 23, No. 9, 1956.
7. Clough, R. W., "The Finite Element Method in Structural Mechanics", Chapter 7, Stress Analysis, O. C. Zienkiewicz & G. S. Holister ed., John Wiley and Sons, Ltd. 1965.
8. Clough, R. W. and Tocher, J. L., "Finite Element Stiffness Matrices for the Analysis of Plate Bending", Proceedings, Conference on Matrix Methods in Structural Mechanics, Air Force Institute of Technology, Wright-Patterson Air Force Base, Ohio, October 1965.
9. Grafton, P. E., and Strome, D. R., "Analysis of Axisymmetrical Shells by the Direct Stiffness Method", AIAA Journal, Vol.1, p. 2342 1963.

10. Clough, R. W., and Tocher, J. L., "Analysis of Thin Arch Dams by the Finite Element Method", Theory of Arch Dams, J. R. Rydzewski, ed., Pergamon Press, 1964.
 11. Clough, R. W. and Johnson, C. P., "A Finite Element Approximation for the Analysis of Thin Shells", submitted to the International Journal of Solids and Structures, Oct. 1966.
 12. DeFries-Skene, A. E., Scordelis, A. C., "Direct Stiffness Solution for Folded Plates", Proc. ASCE, Vol. 90, Structural Division, ST4, August 1964, pp. 15-47.
- See also:
- Scordelis, A. C. and Lo, K. S., "Computer Analysis of Cylindrical Shells", ACI Journal, Proceedings Vol. 61, No. 5, May 1964, pp. 539-561.
 13. Clough, R. W. and Greste, O. I., "Finite Element Analysis of Tubular Joints", Structures and Materials Research, Department of Civil Engineering, University of California, Berkeley, Preliminary Report to Standard Oil Company of California, November 1966.
 14. Bijlaard, P. P., "Stresses from Local Loadings in Cylindrical Pressure Vessels", Transactions ASME, Vol. 77, No. 6, 1966.

LIST OF FIGURES

- 1 Geometry and Loading of Joints Analyzed
- 2 Allowable Load Types for Case S
- 3 Finite Element Idealization for Tee-Joints
- 4 Finite Element Idealization for Y and K Joints
- 5 Notation for Presentation of Results
- 6 Finite Element-Case S: Displacements, Joint T-1
- 7 Finite Element-Case S: Radial Displacements, Joints T-3, T-4
- 8 Finite Element-Case S: Tangential Displacements, Joints T-3, T-4
- 9 Finite Element-Case S: Moments, Joint T-1
- 10 Finite Element-Case S: Moments, Joints T-3, T-4
- 11 Finite Element-Case S: Membrane Forces, Joint T-1
- 12 Finite Element-Case S: Membrane Forces, Joints T-3, T-4
- 13 Line Load-Branch Case: Displacements, Joint T-1
- 14 Line Load-Branch Case: Radial Displacements, Joints T-3, T-4
- 15 Line Load-Branch Case: Tangential Displacements, Joints T-3, T-4
- 16 Line Load-Branch Case: Moments, Joint T-1
- 17 Line Load-Branch Case: Moments, Joints T-3, T-4
- 18 Line Load-Branch Case: Membrane Forces, Joint T-1
- 19 Line Load-Branch Case: Membrane Forces, Joints T-3, T-4
- 20 Surface Stresses at Center Section, Joints T-1, T-3, T-4
- 21 Surface Stresses along Top of Chord, Joints T-1, T-3, T-4
- 22 Principal Stresses at Pipe Intersection, Joints T-1, T-3, T-4
- 23 Surface Stresses at Center Section, Joint T-2
- 24 Surface Stresses along Y-Axis, Joint T-2

- 25 Vertical Displacements along Y-Axis, Joint T-2
- 26 Vertical Displacements along Y-Axis, Joints Y and K
- 27 Surface Stresses along Y-Axis, Joints Y and K
- 28 Principal Stresses at Pipe Intersection, Joints Y and K

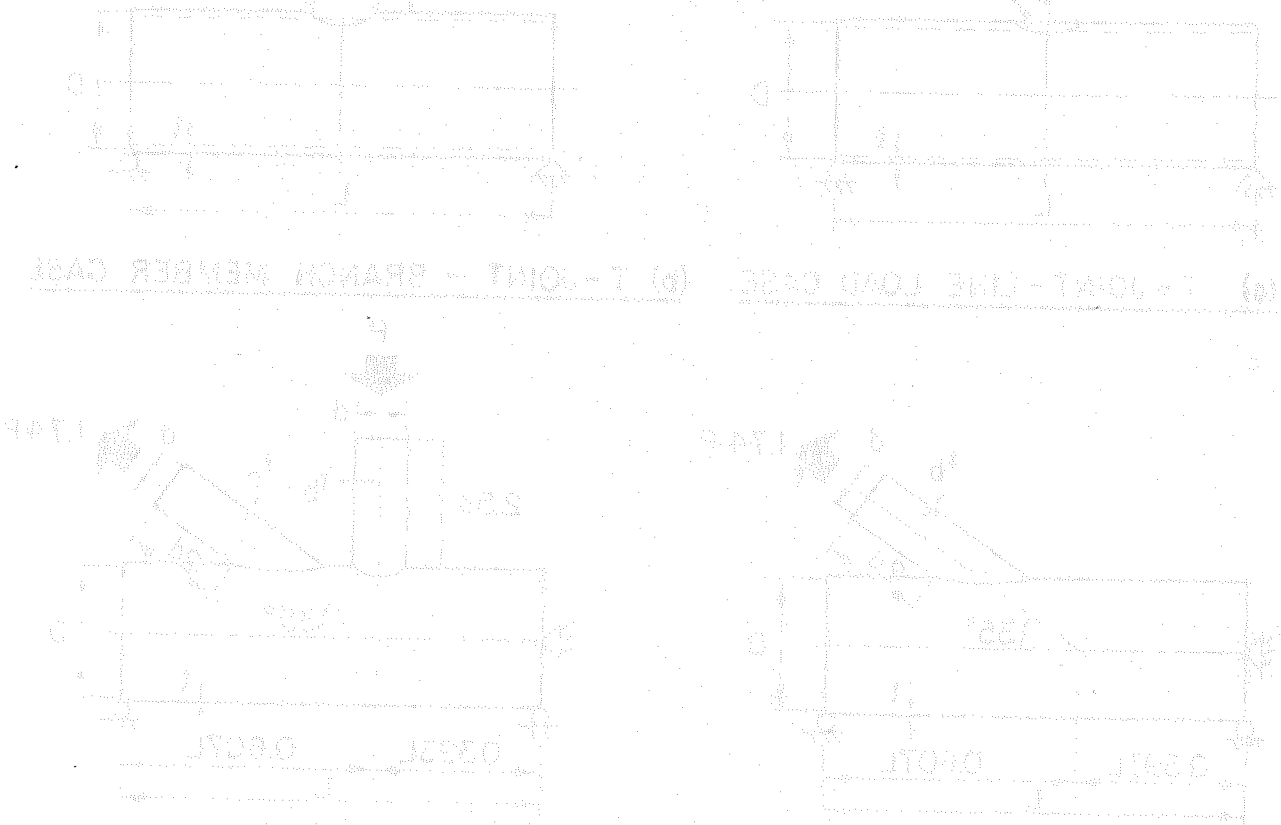


FIG. 1 GEOMETRY AND LOADING OF JOINTS ANALYZED

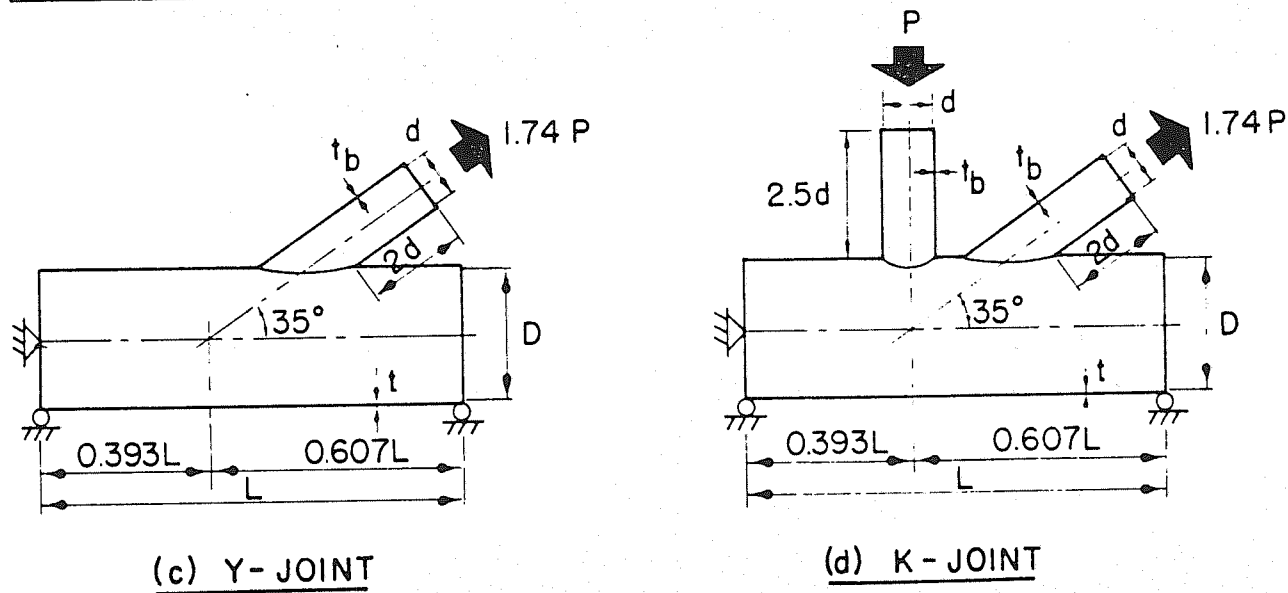
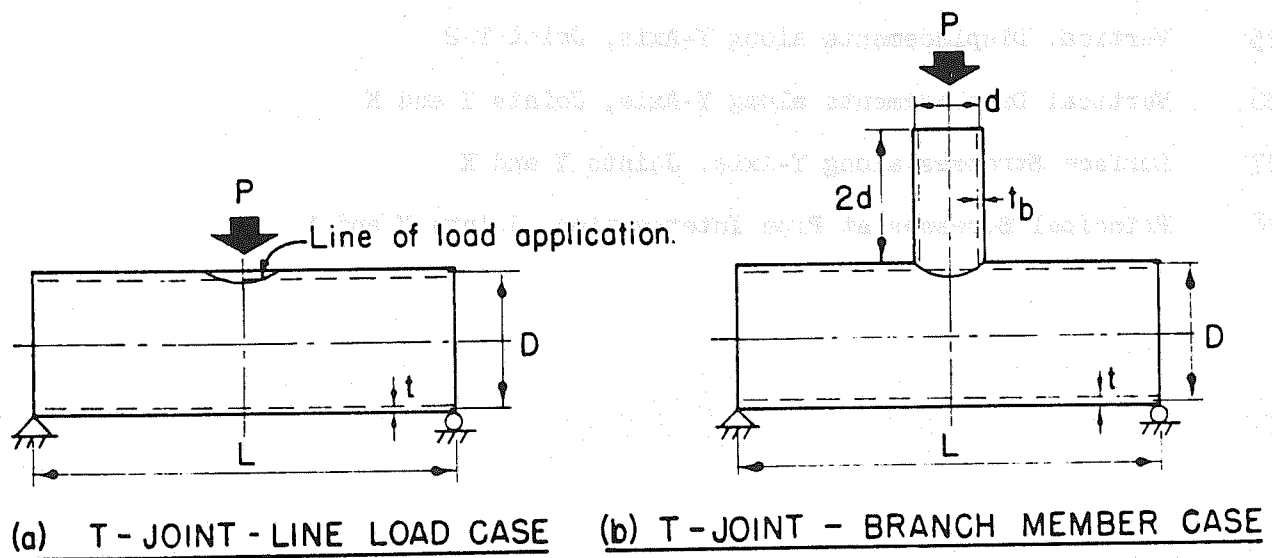


FIG. 1 GEOMETRY AND LOADING OF JOINTS ANALYZED

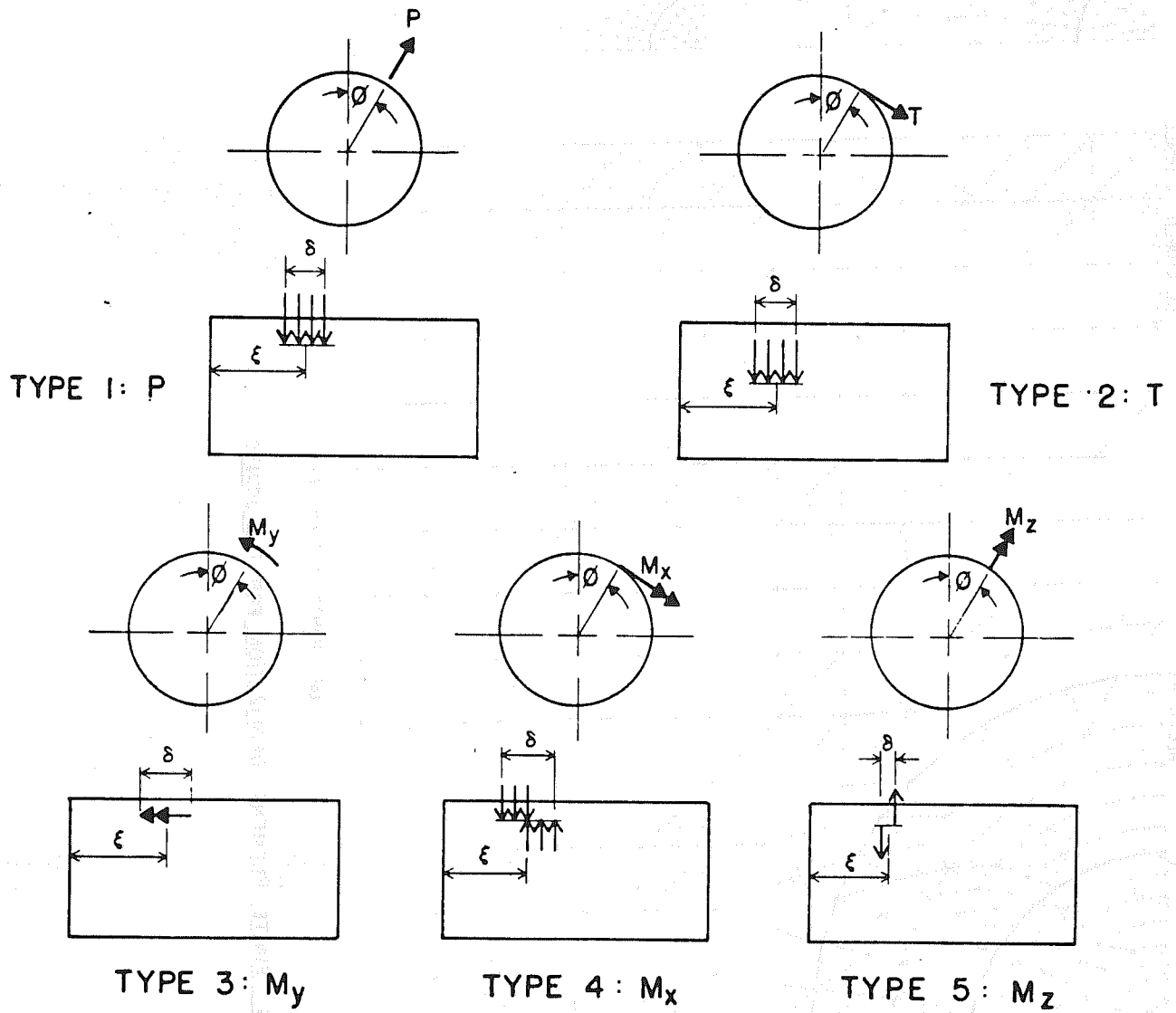
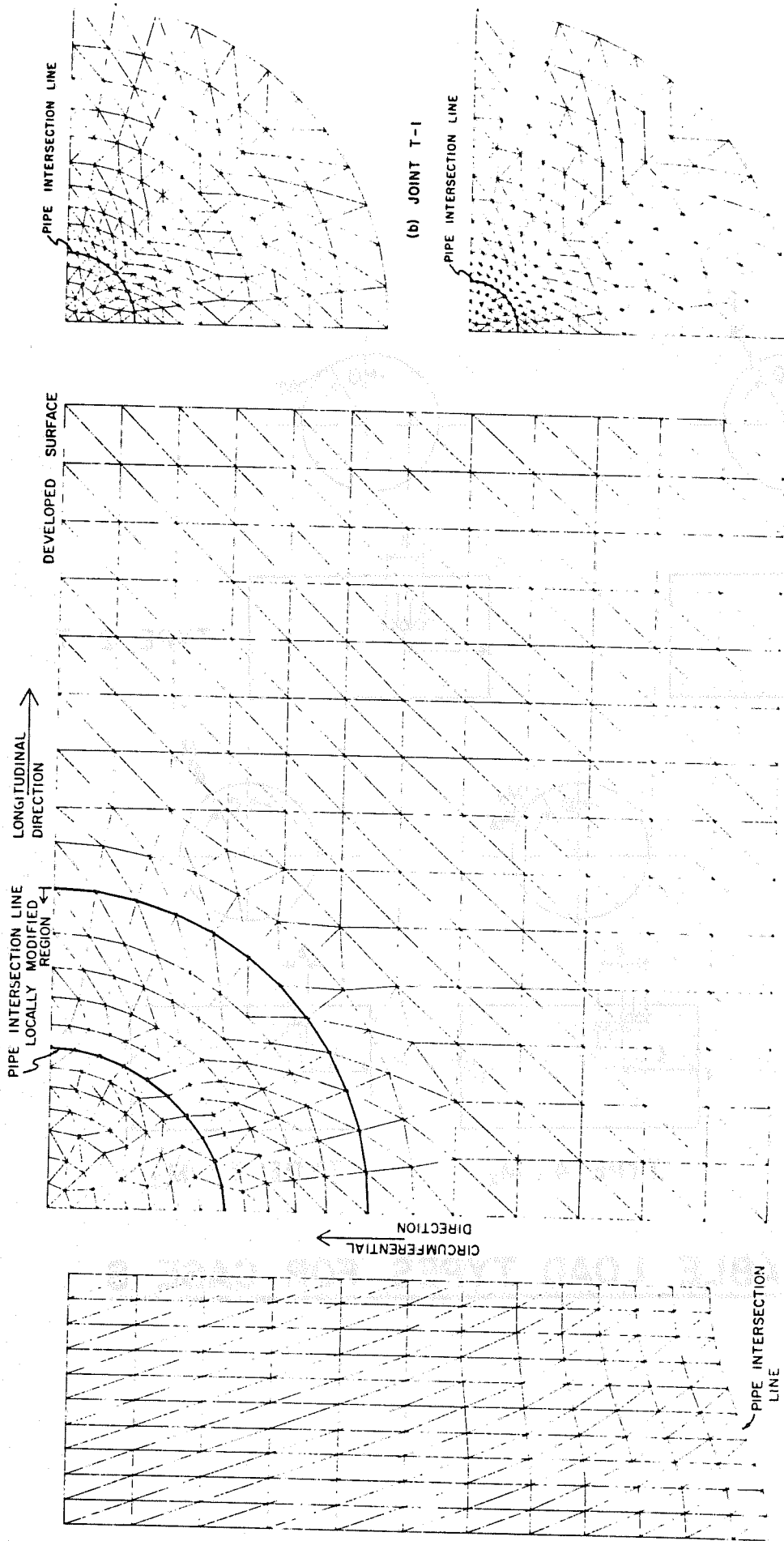


FIG. 2 ALLOWABLE LOAD TYPES FOR CASE S



(a) JOINTS T-3 AND T-4

FIG. 3 FINITE ELEMENT IDEALIZATION FOR TEE JOINTS

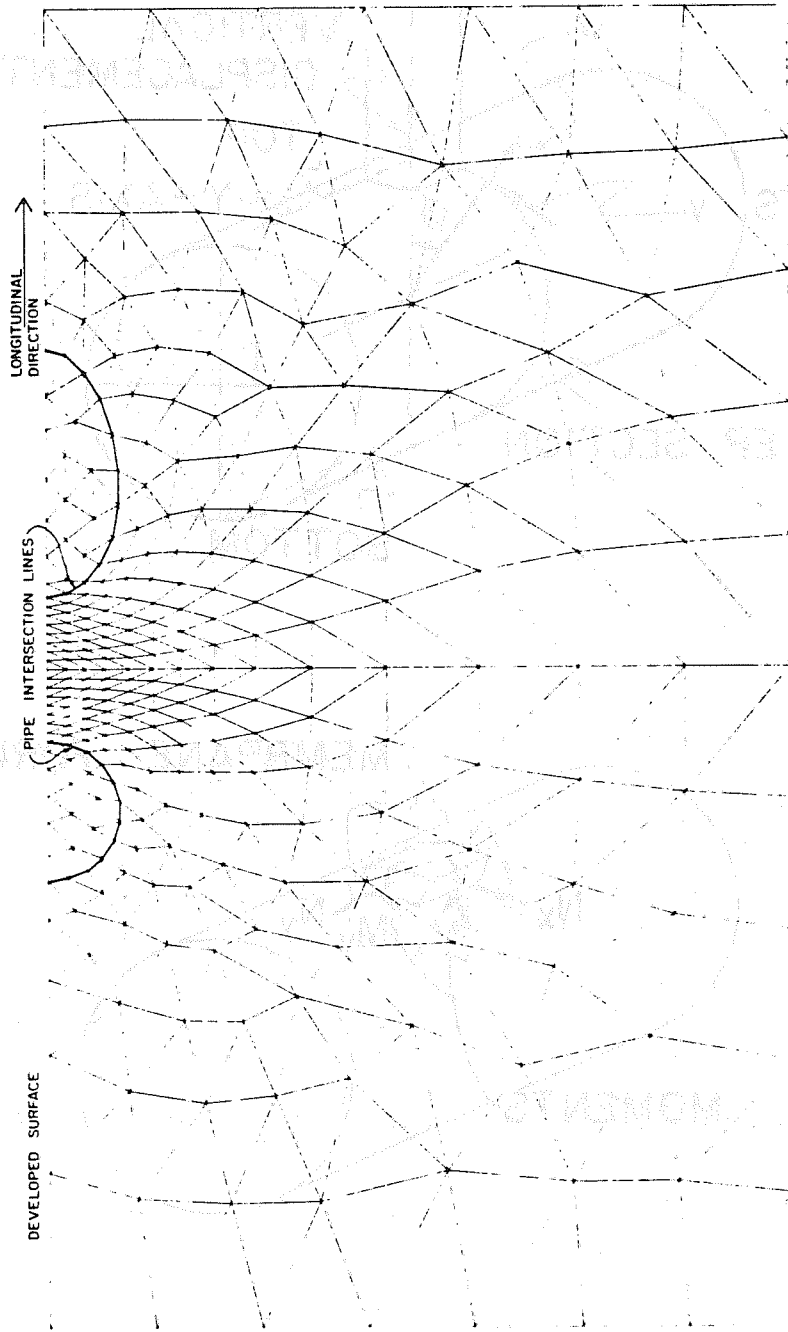
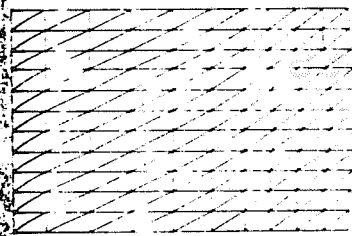
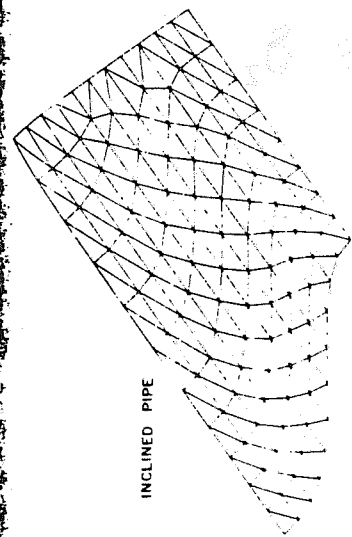


FIG. 4 FINITE ELEMENT IDEALIZATION FOR Y AND K JOINTS

FIG. 5 NOTATION FOR PRESENTATION OF RESULTS

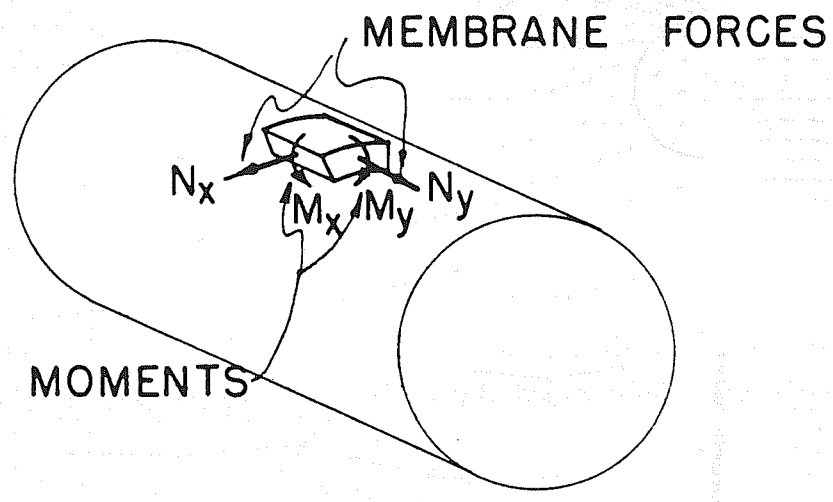
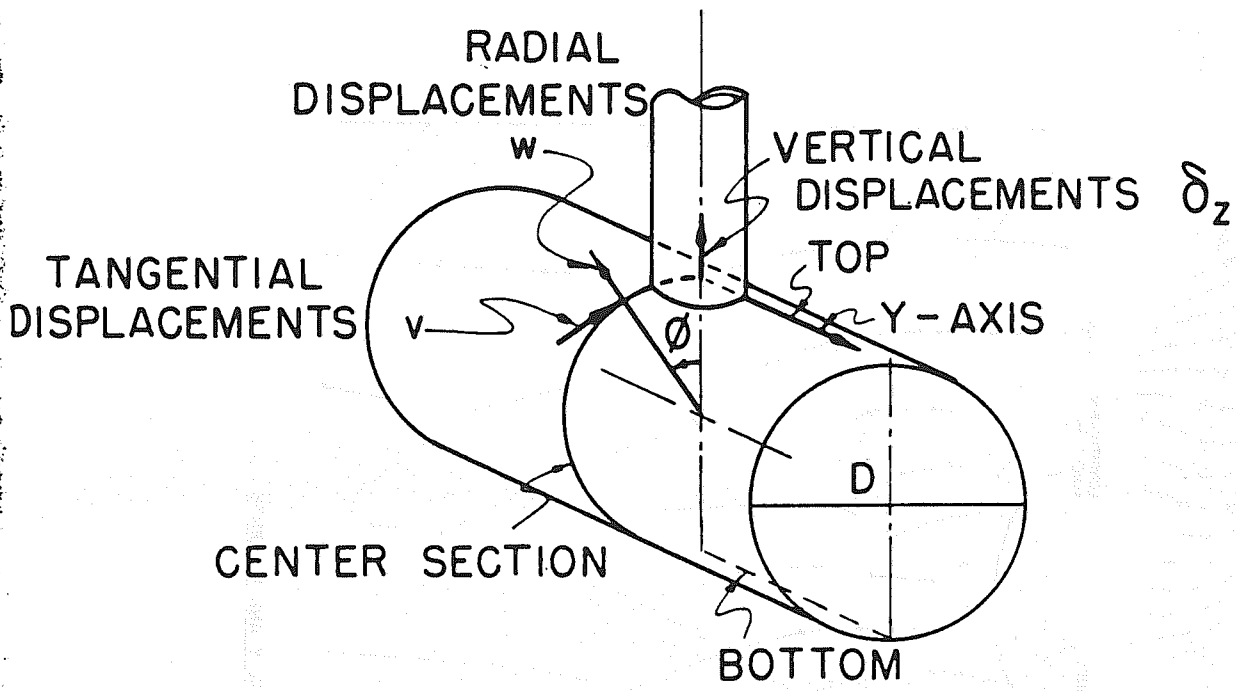
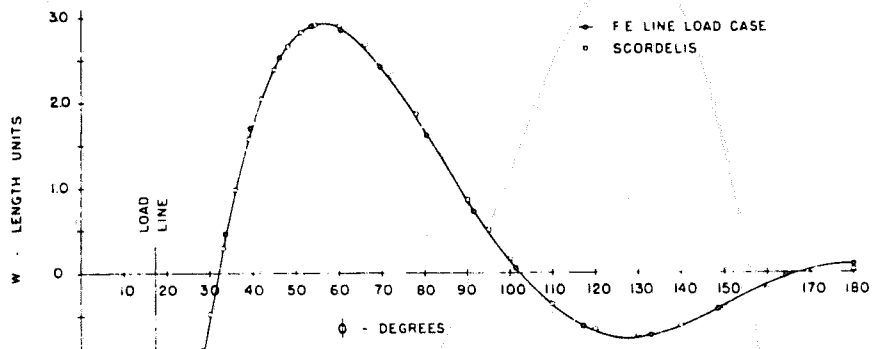
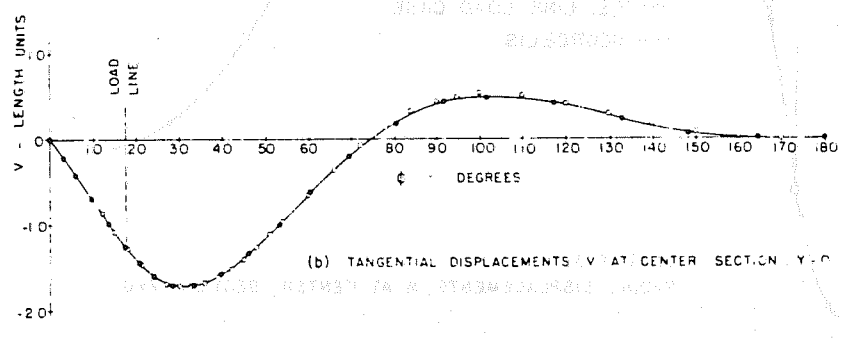


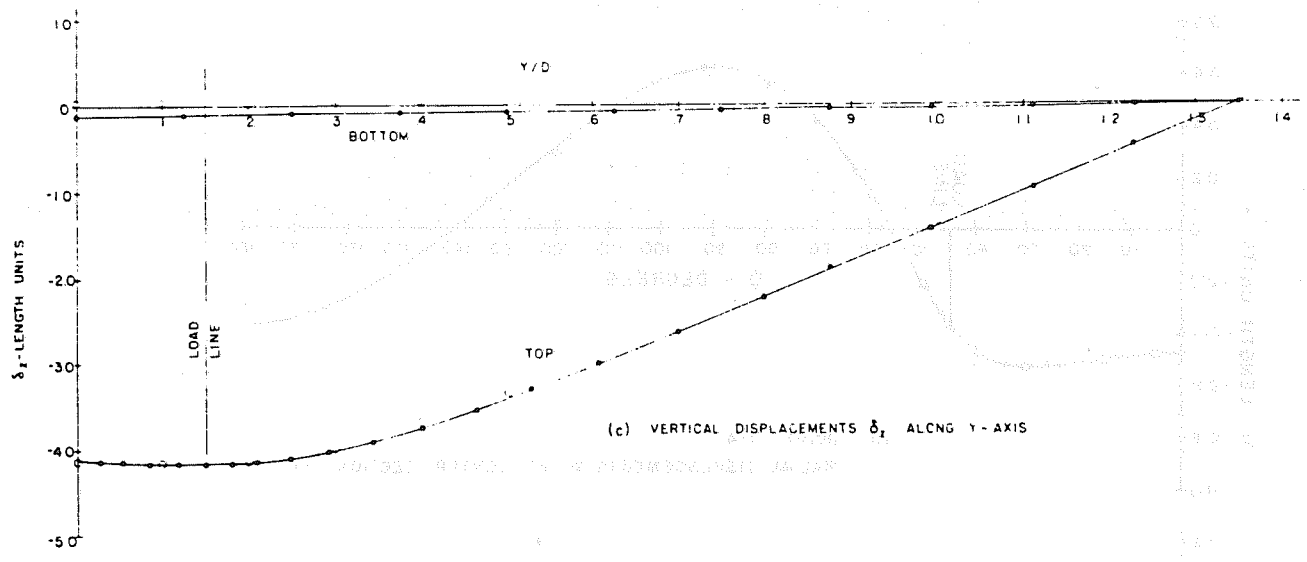
FIG. 5. NOTATION FOR PRESENTATION OF RESULTS



(a) RADIAL DISPLACEMENTS w AT CENTER SECTION $y=0$



(b) TANGENTIAL DISPLACEMENTS v AT CENTER SECTION $y=0$



(c) VERTICAL DISPLACEMENTS δ_1 ALONG y -AXIS

FIG. 6. FINITE ELEMENT-CASE S DISPLACEMENTS, JOINT T-1

FIG. 7. FINITE ELEMENT-CASE S
RADIAL DISPLACEMENTS, JOINTS T-2 AND T-4

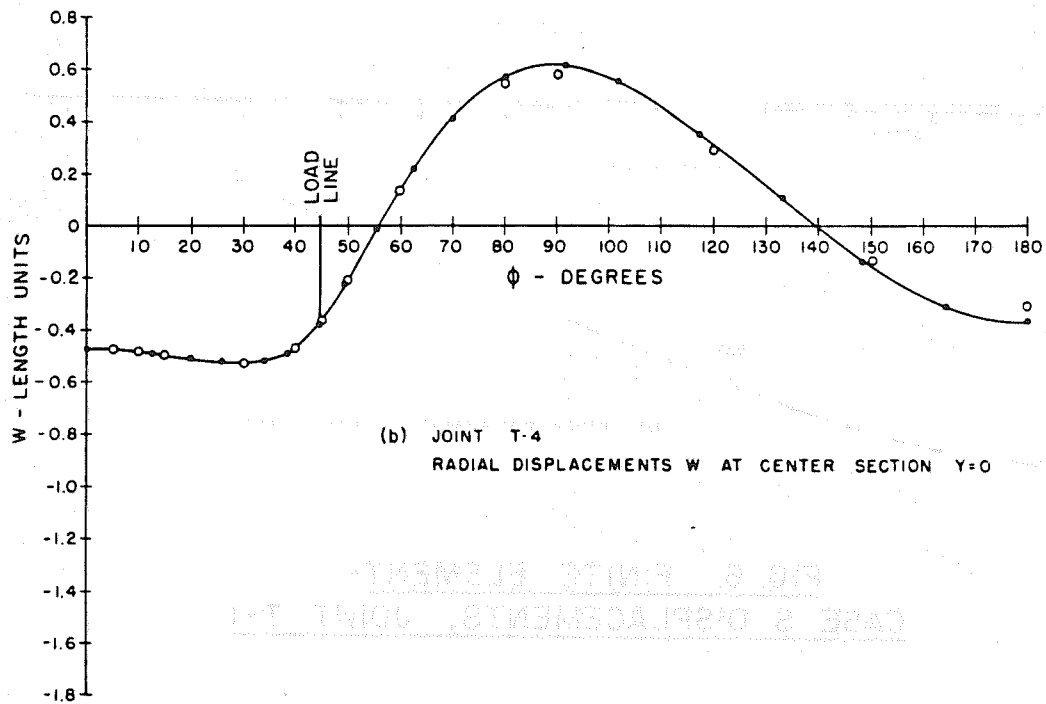
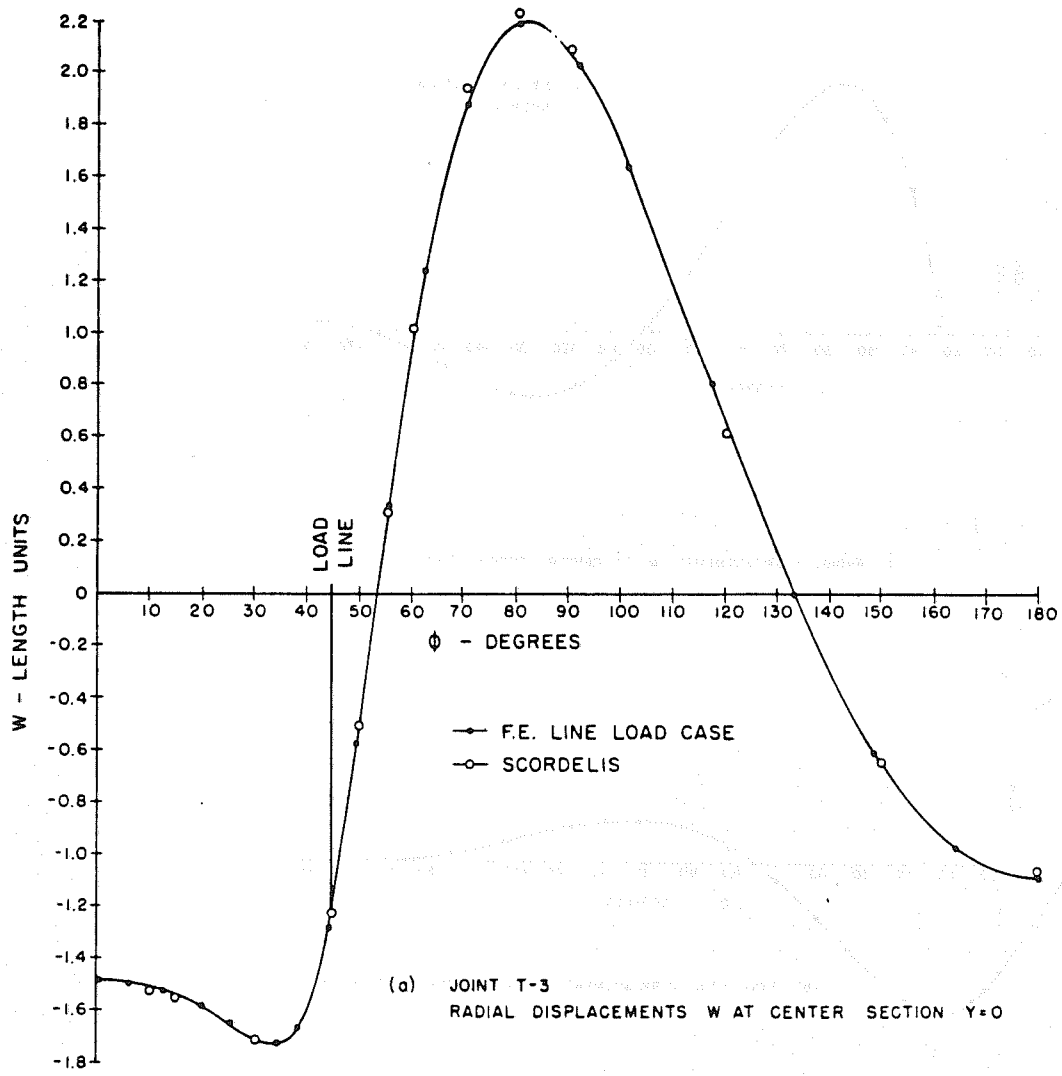
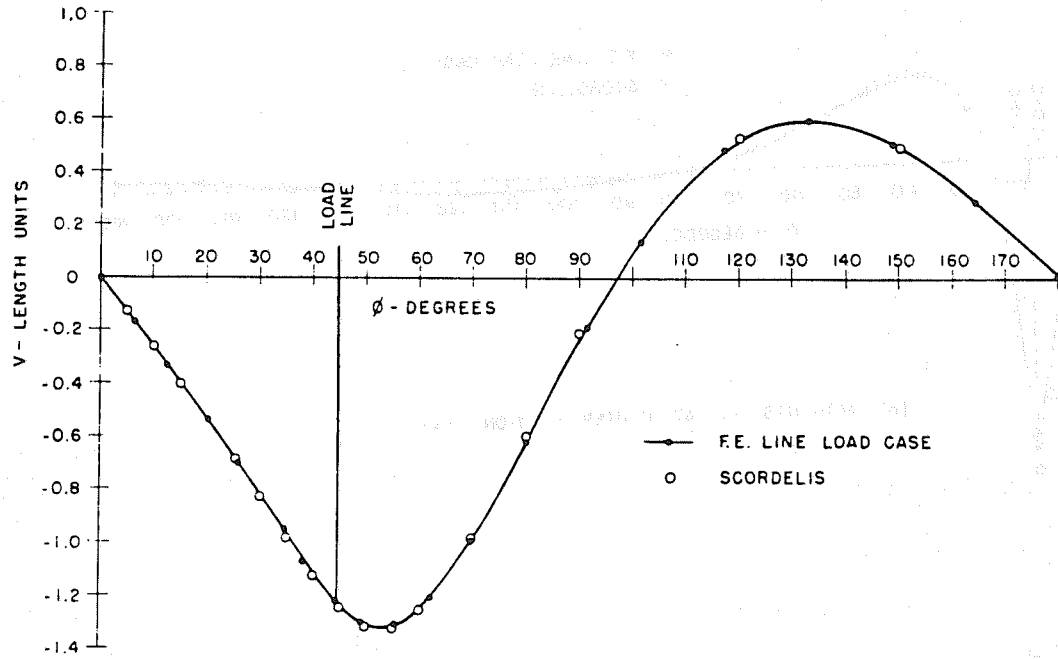
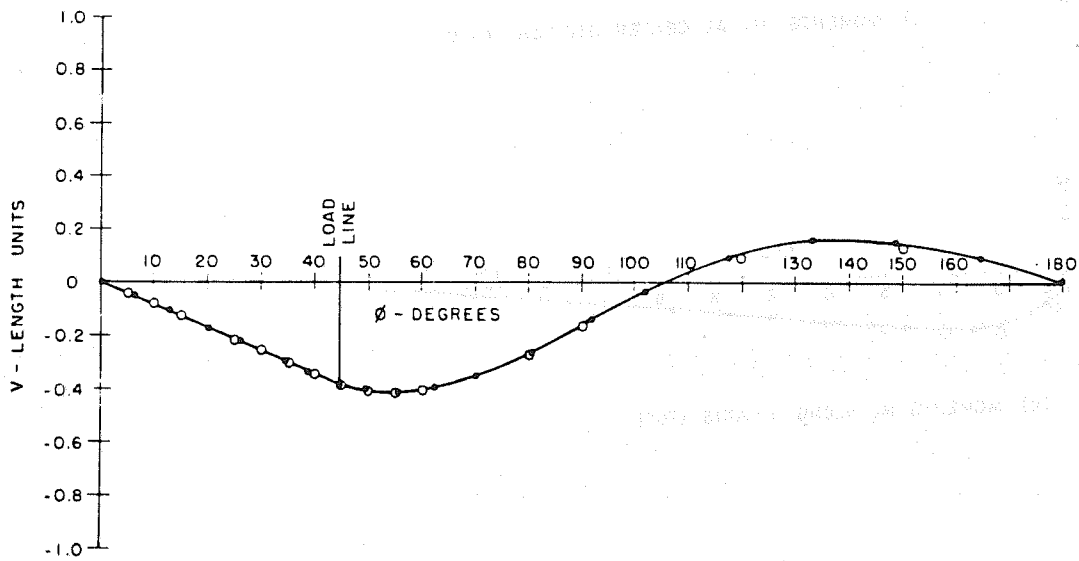


FIG. 7. FINITE ELEMENT - CASE S
RADIAL DISPLACEMENTS, JOINTS T-3 AND T-4



(a) JOINT T-3
TANGENTIAL DISPLACEMENTS V AT CENTER SECTION Y=0



(b) JOINT T-4
TANGENTIAL DISPLACEMENT V AT CENTER SECTION Y=0

FIG. 8 FINITE ELEMENT - CASE S TANGENTIAL DISPLACEMENTS, JOINTS T-3 AND T-4

FIG. 8 FINITE ELEMENT - CASE S TANGENTIAL DISPLACEMENTS, JOINTS T-3 AND T-4

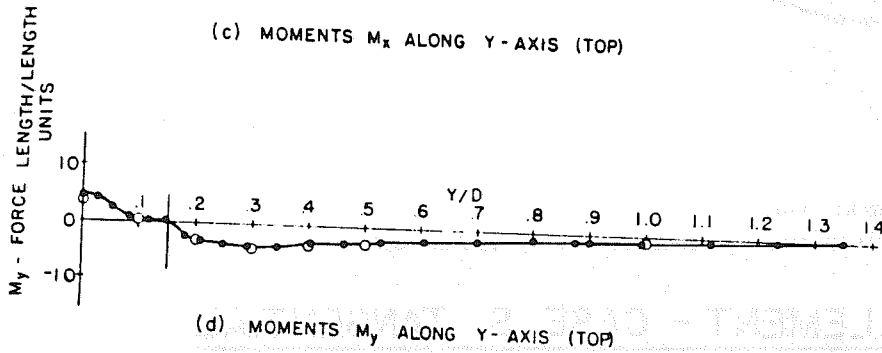
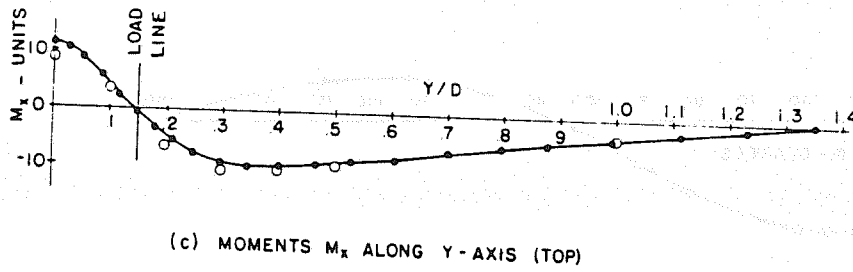
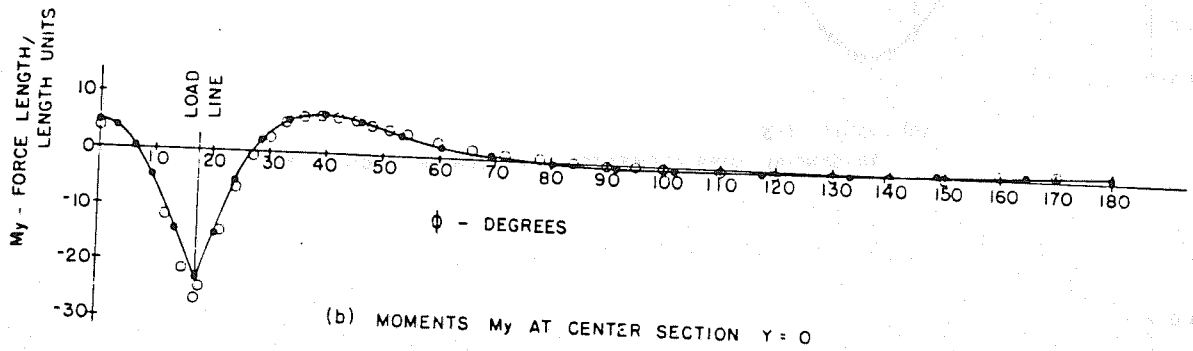
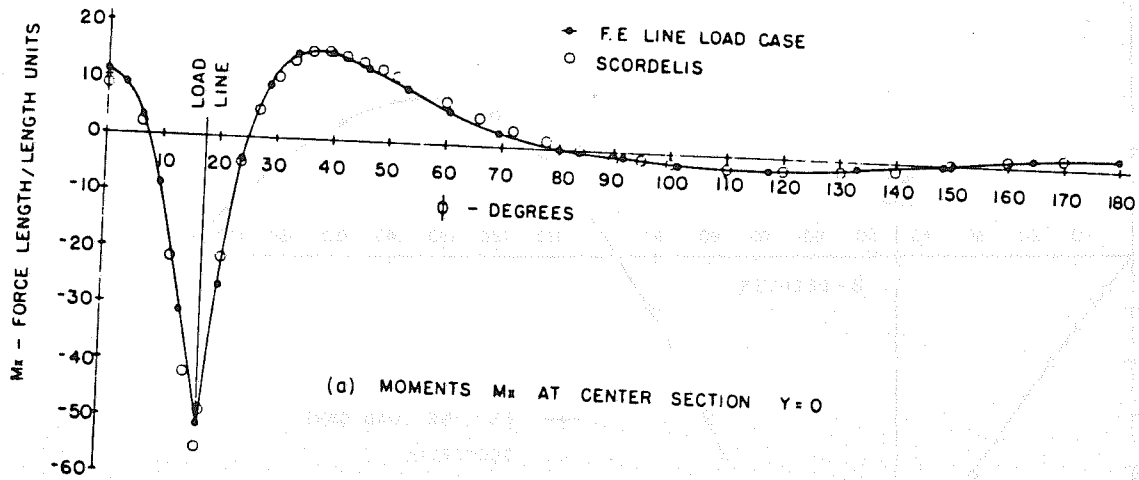


FIG. 9 FINITE ELEMENT - CASE S MOMENTS, JOINT T-1

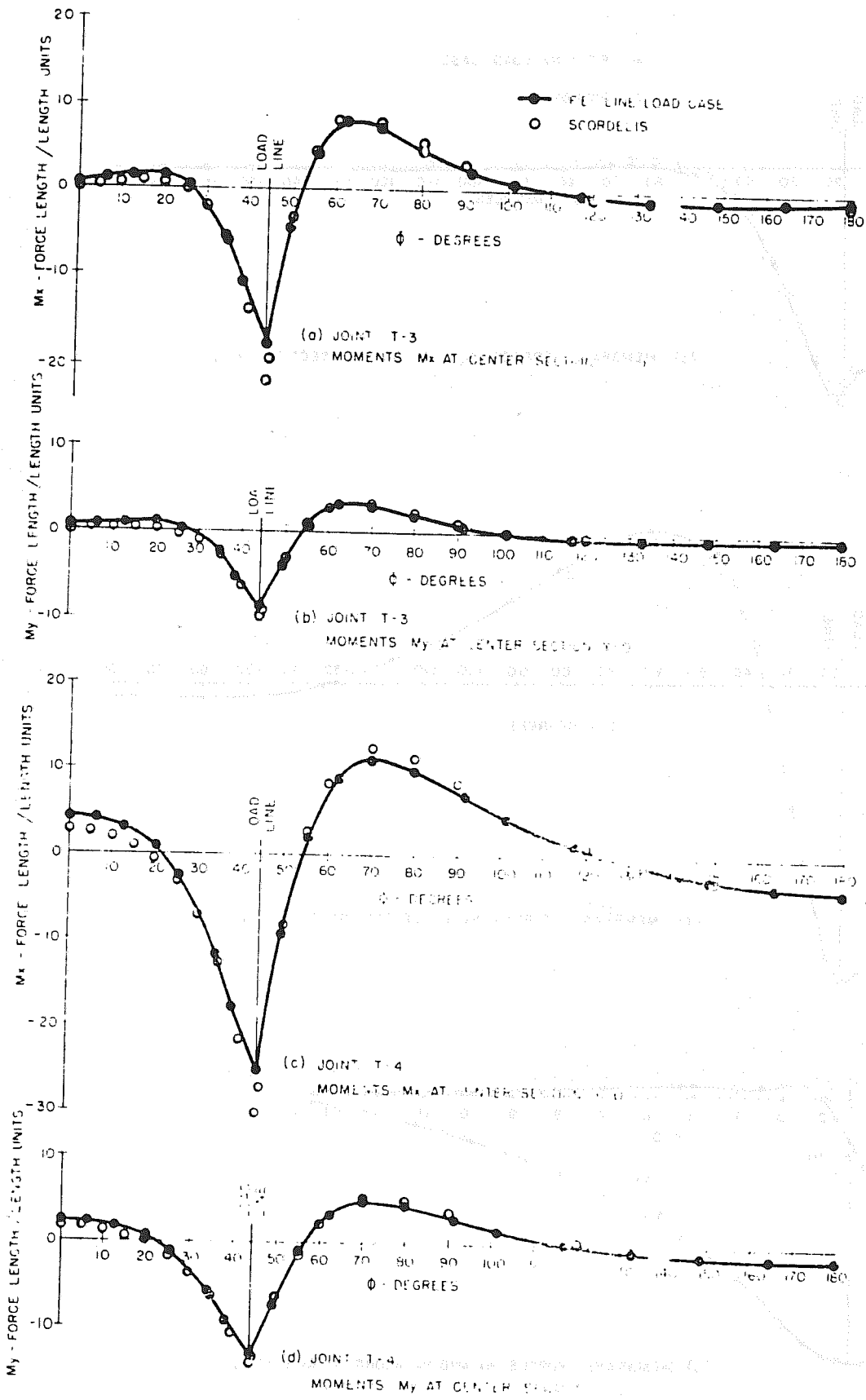


FIG. 10 FINITE ELEMENT - CASE S
MOMENTS, JOINTS T-3 AND T-4

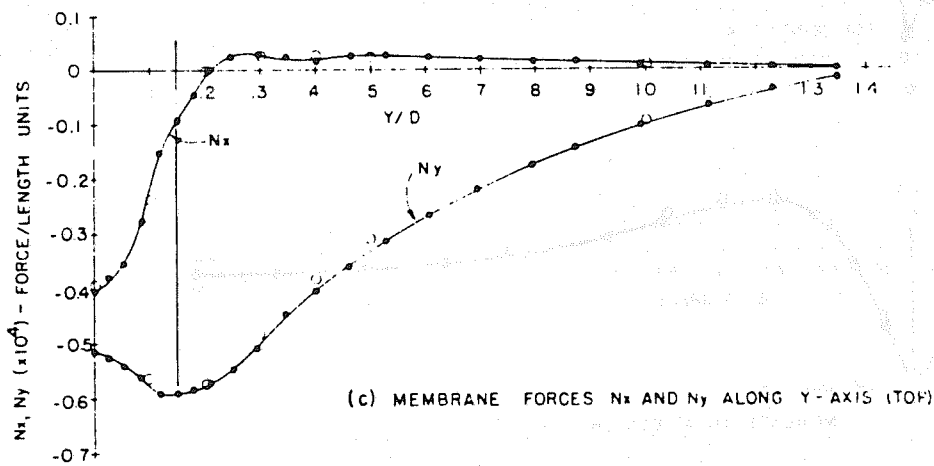
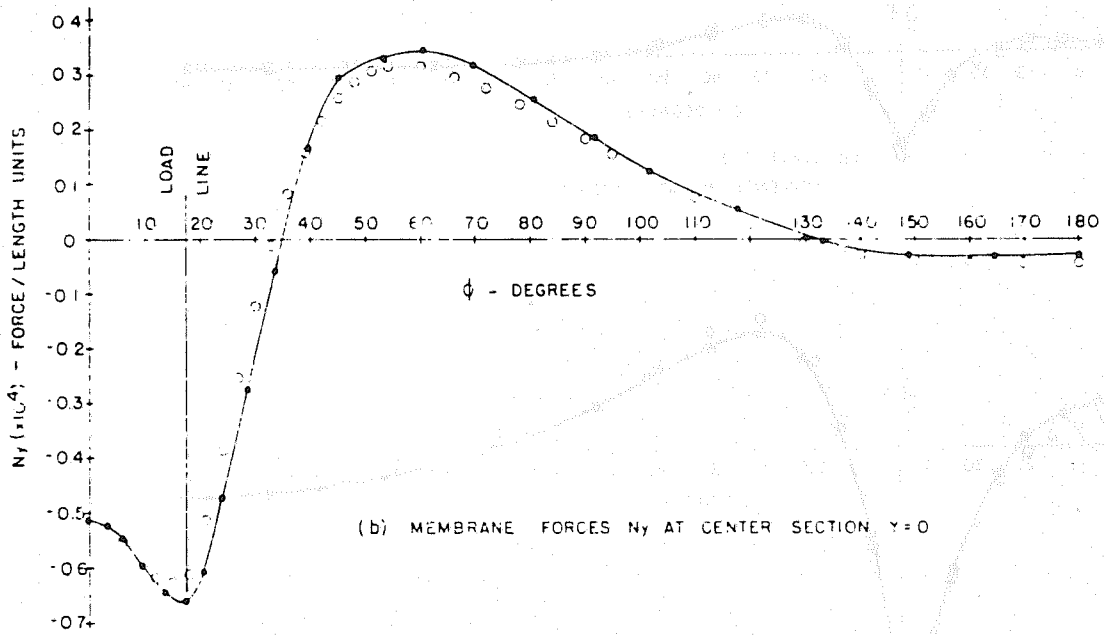
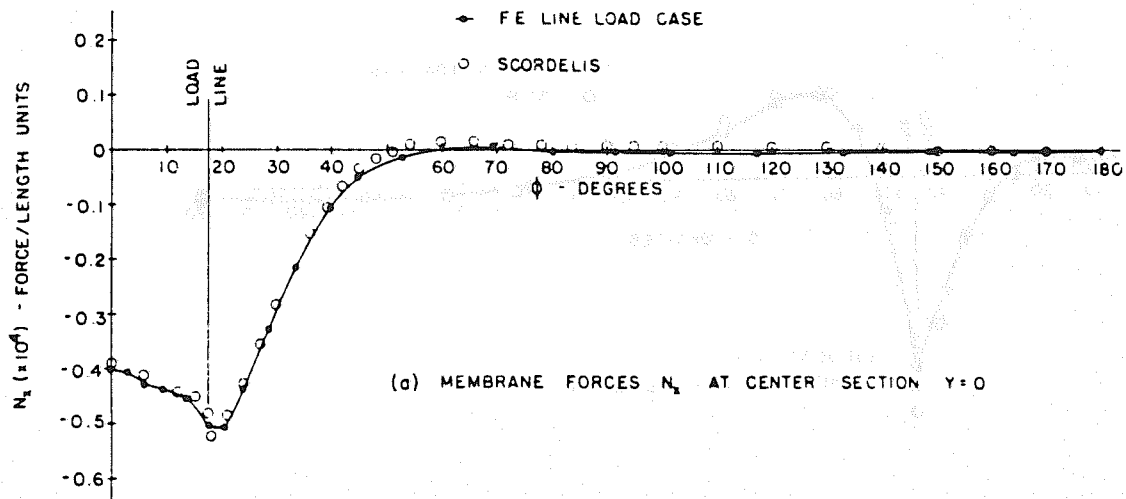
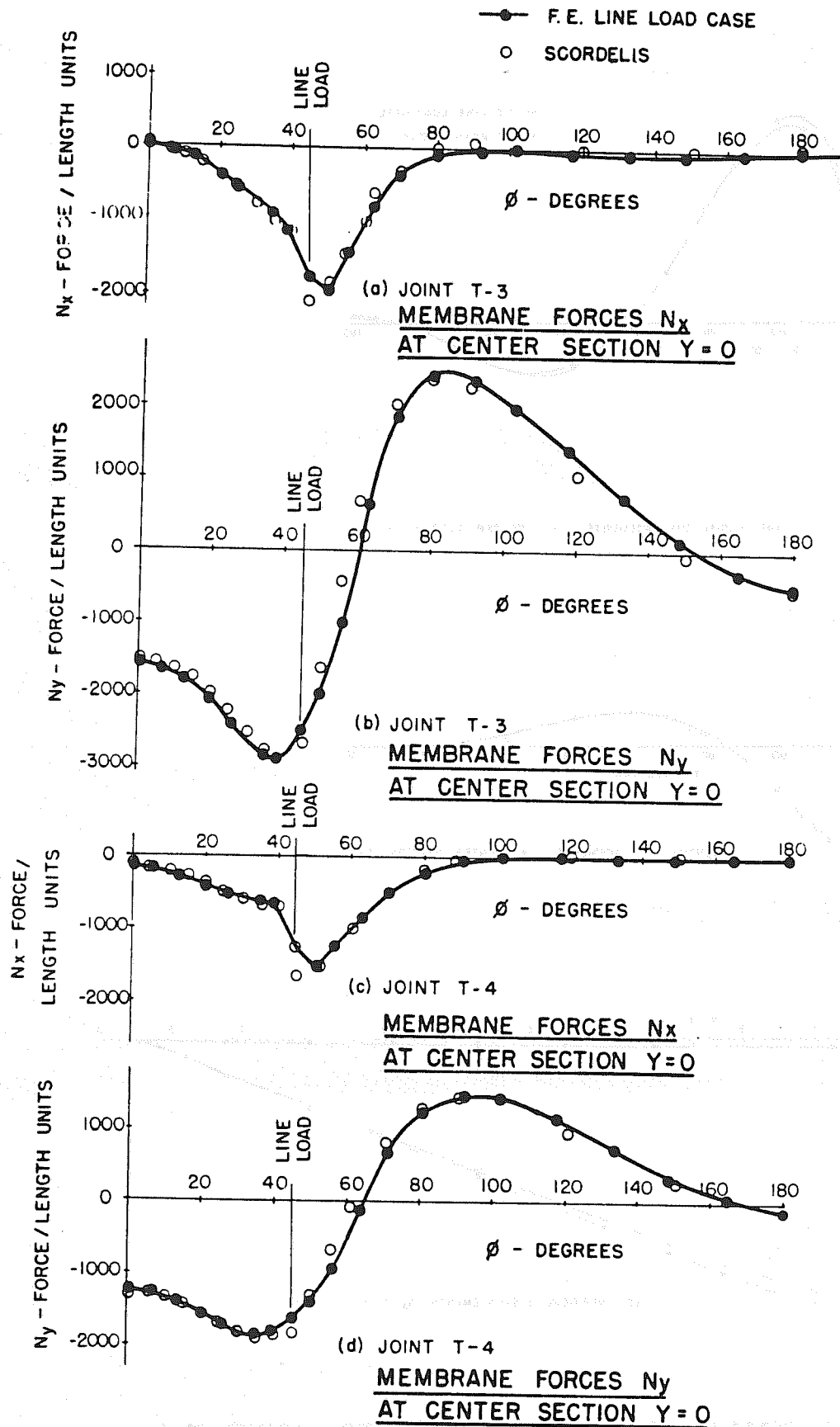
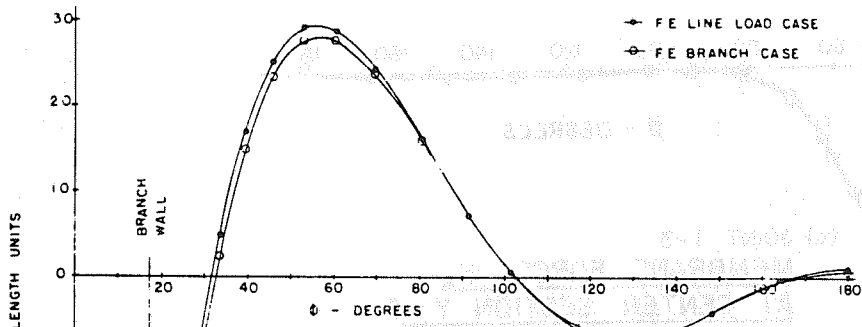


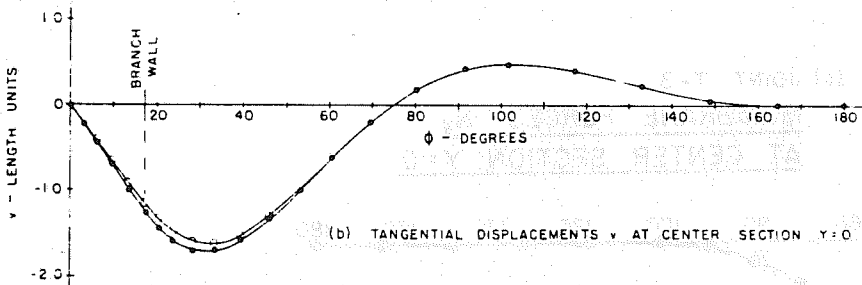
FIG. II FINITE ELEMENT - CASE S
MEMBRANE FORCES, JOINT T-1



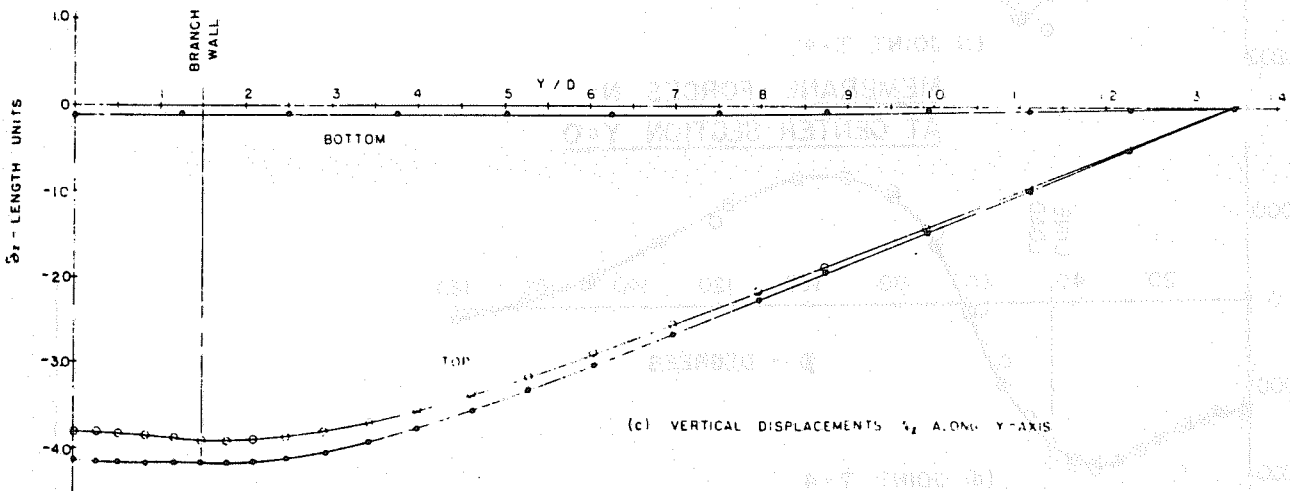
**FIG. 12 FINITE ELEMENT - CASE S
 MEMBRANE FORCES, JOINTS T-3 AND T-4**



(a) RADIAL DISPLACEMENTS w AT CENTER SECTION $y = 0$



(b) TANGENTIAL DISPLACEMENTS v AT CENTER SECTION $y = 0$



(c) VERTICAL DISPLACEMENTS w_z ALONG Y-AXIS

FIG. 13 LINE LOAD-BRANCH CASE DISPLACEMENTS, JOINT T-1

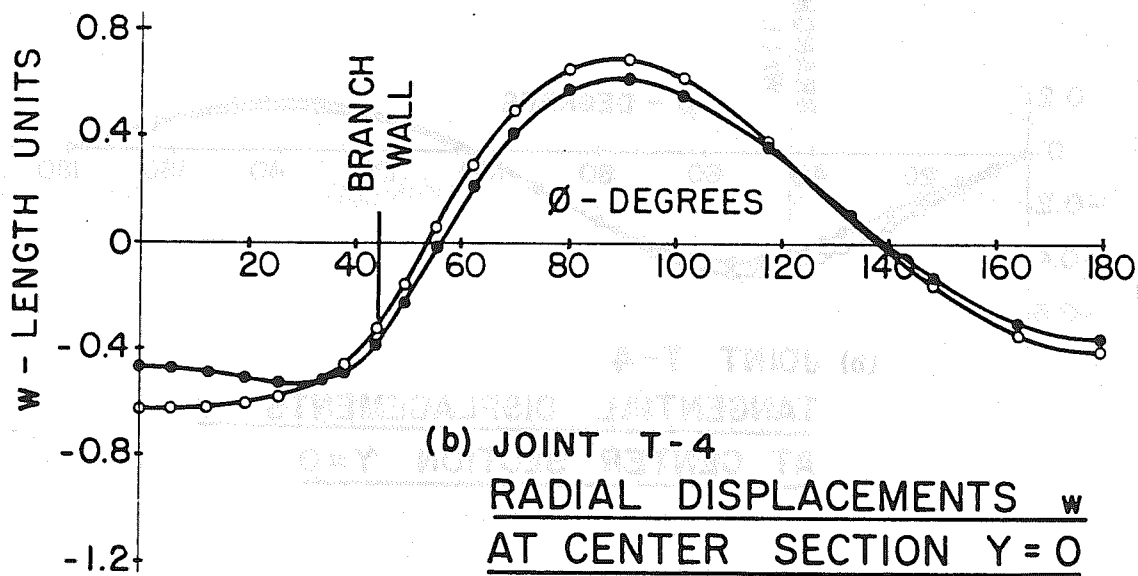
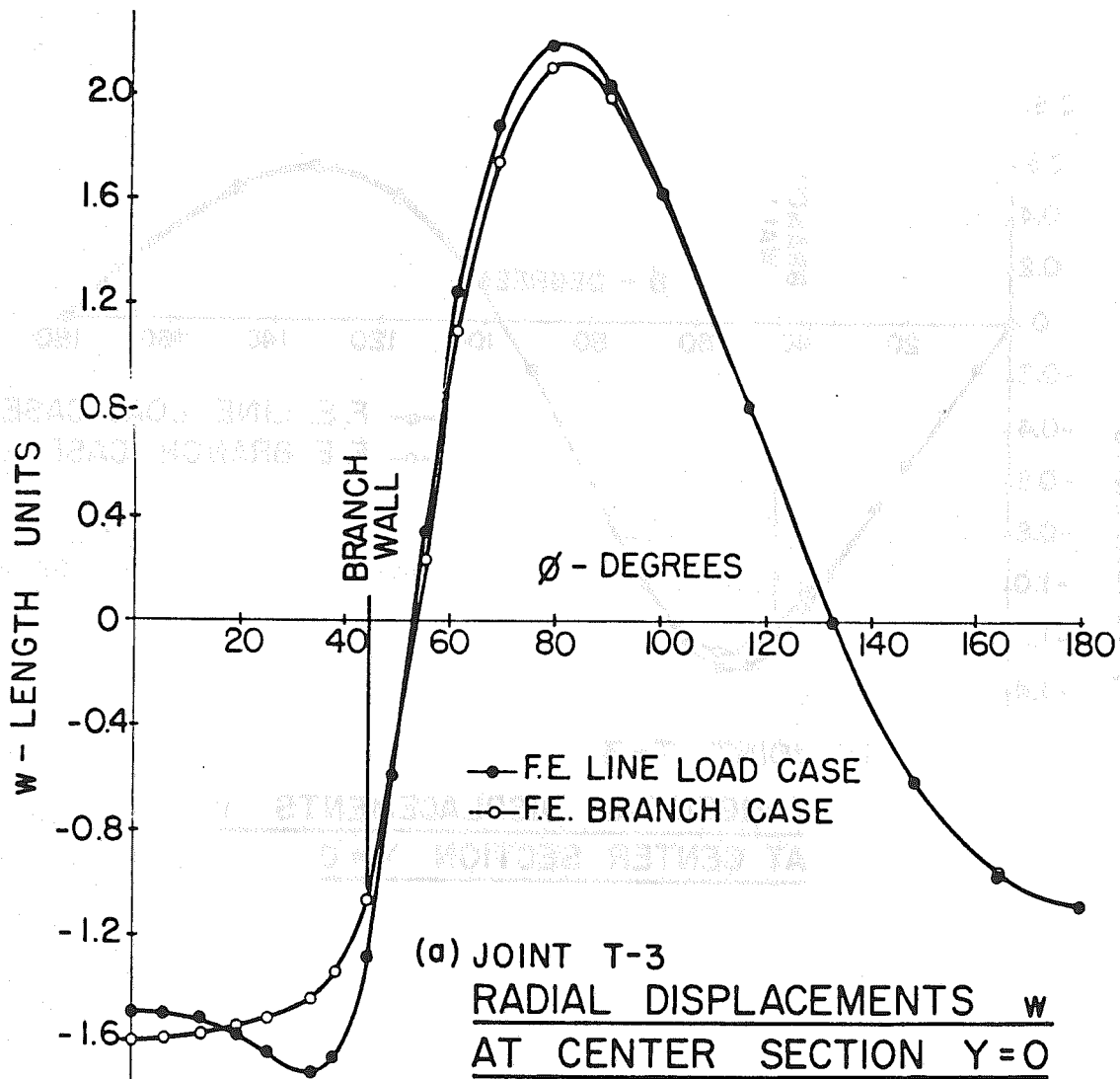
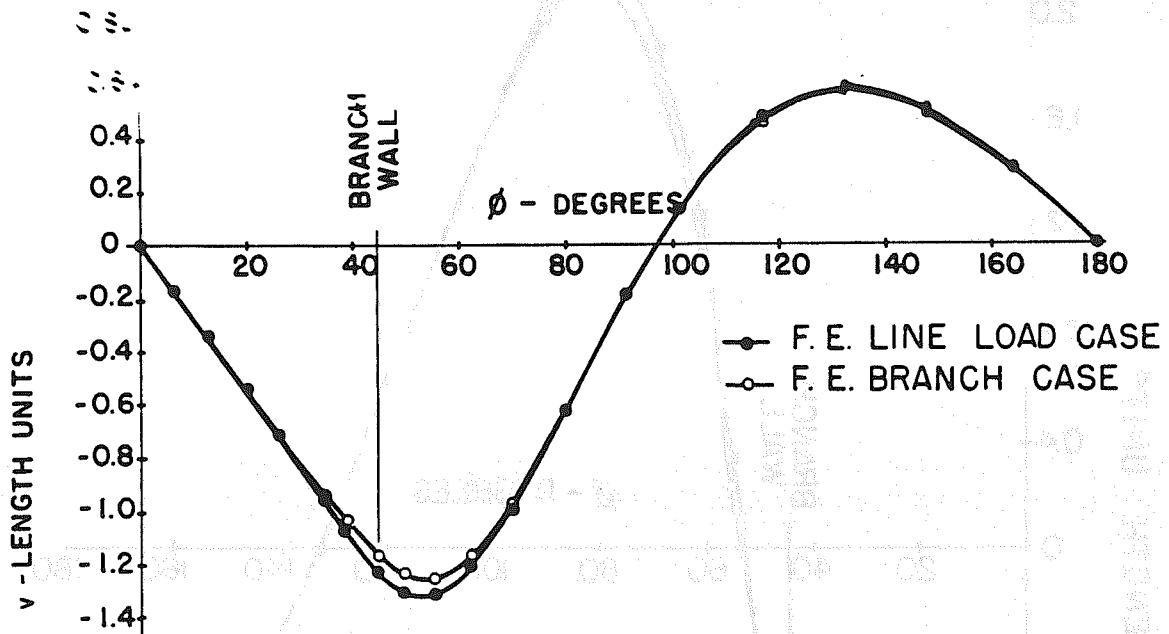
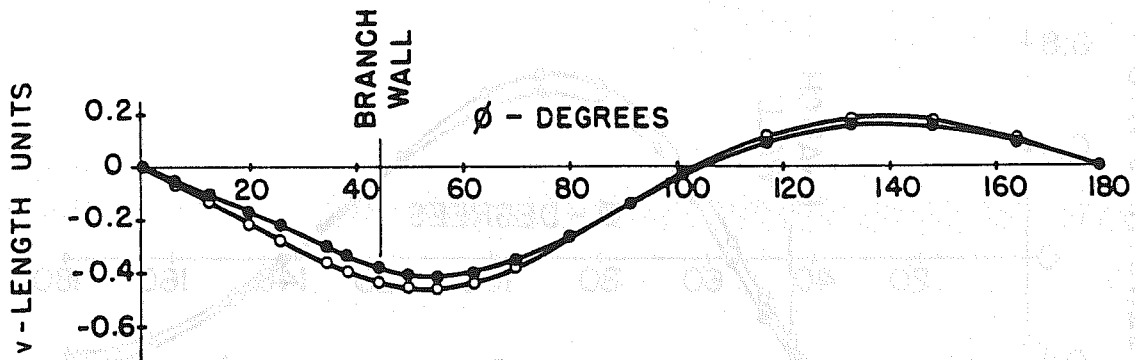


FIG. 14 LINE LOAD - BRANCH CASE
RADIAL DISPLACEMENTS, JOINTS T-3 AND T-4



(a) JOINT T-3
TANGENTIAL DISPLACEMENTS v
AT CENTER SECTION $Y = 0$



(b) JOINT T-4
TANGENTIAL DISPLACEMENTS v
AT CENTER SECTION $Y = 0$

FIG. 15 LINE LOAD - BRANCH CASE TANGENTIAL DISPLACEMENTS, JOINTS T-3 AND T-4

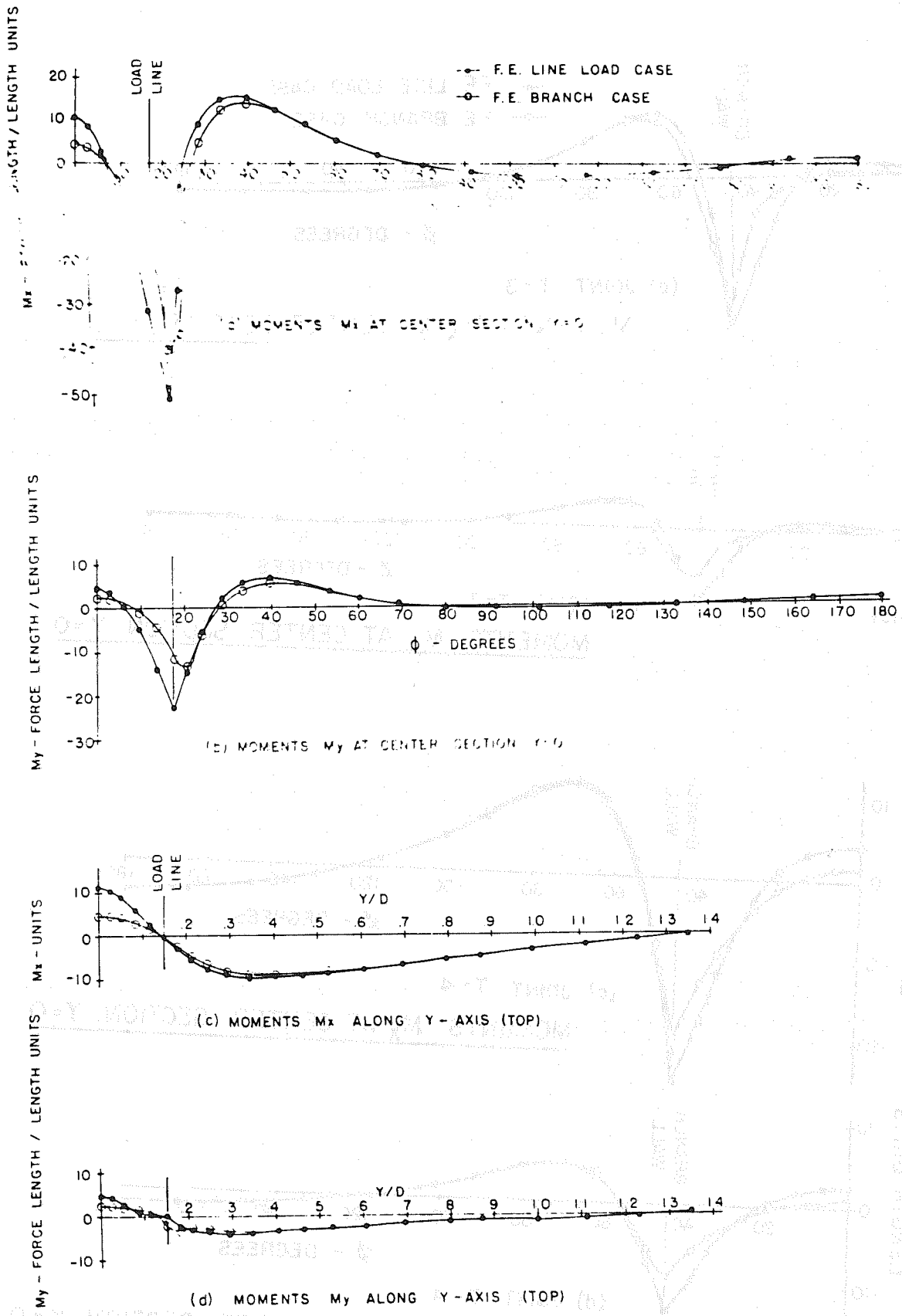


FIG. 16 LINE LOAD - BRANCH CASE
MOMENTS, JOINT T-1

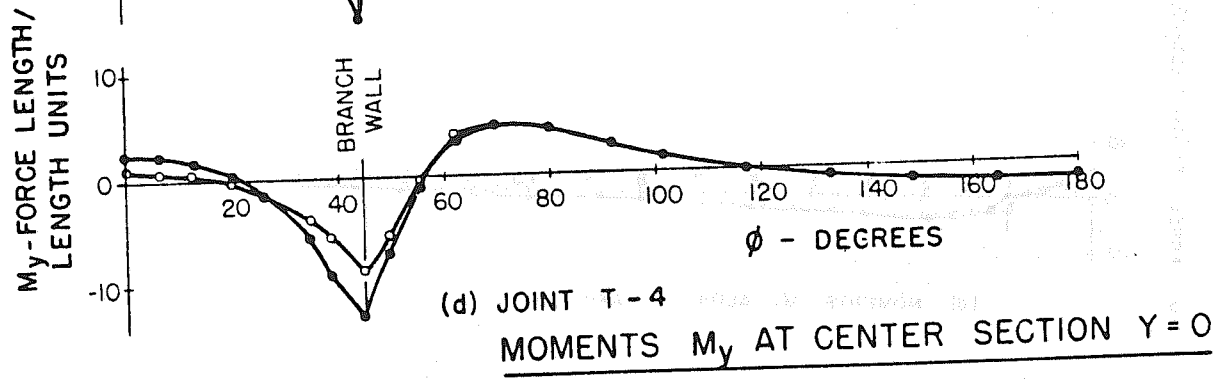
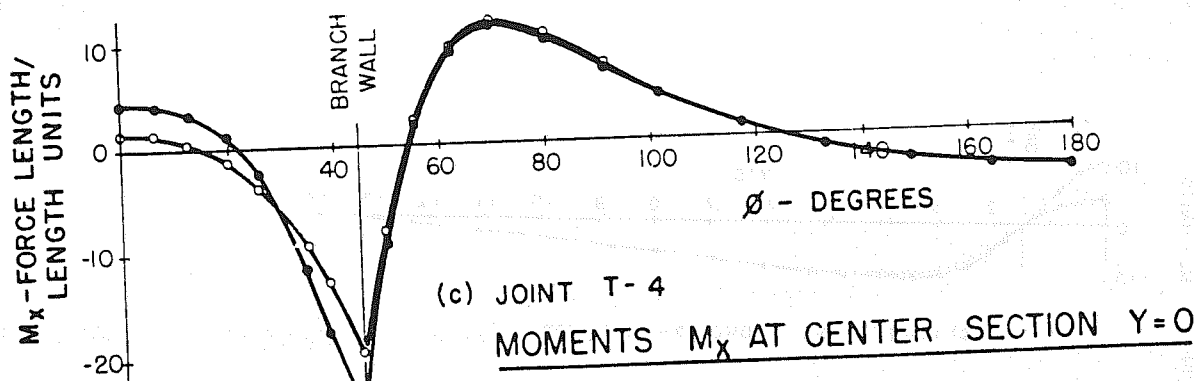
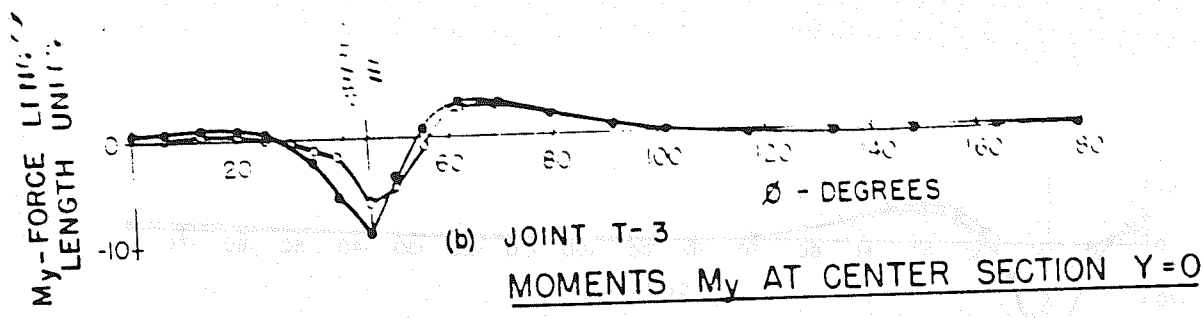
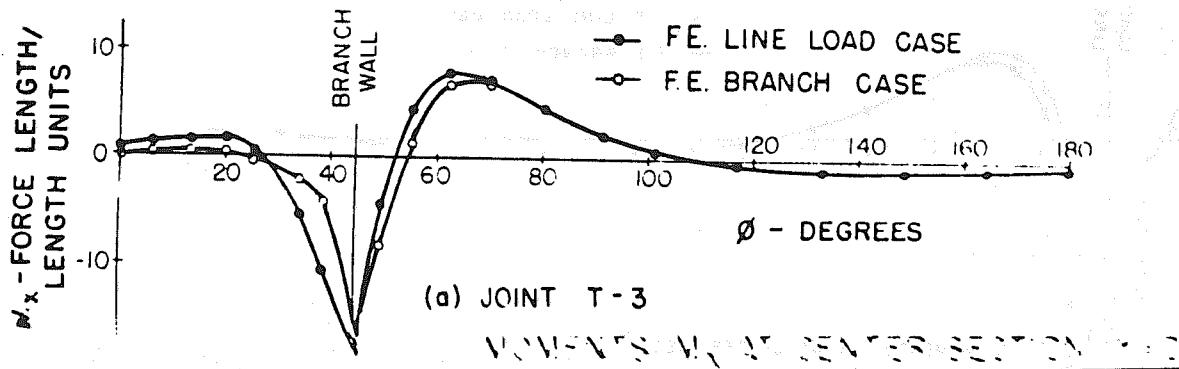


FIG. 17 LINE LOAD - BRANCH CASE
MOMENTS, JOINTS T-3 AND T-4

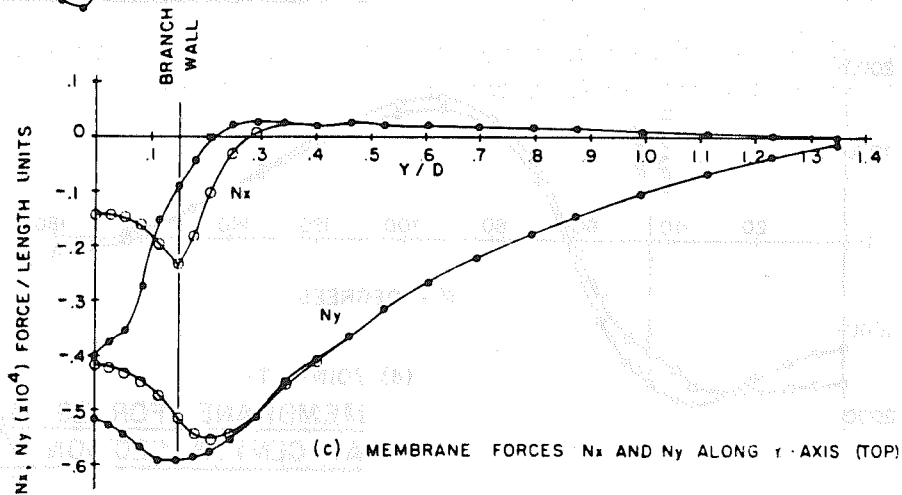
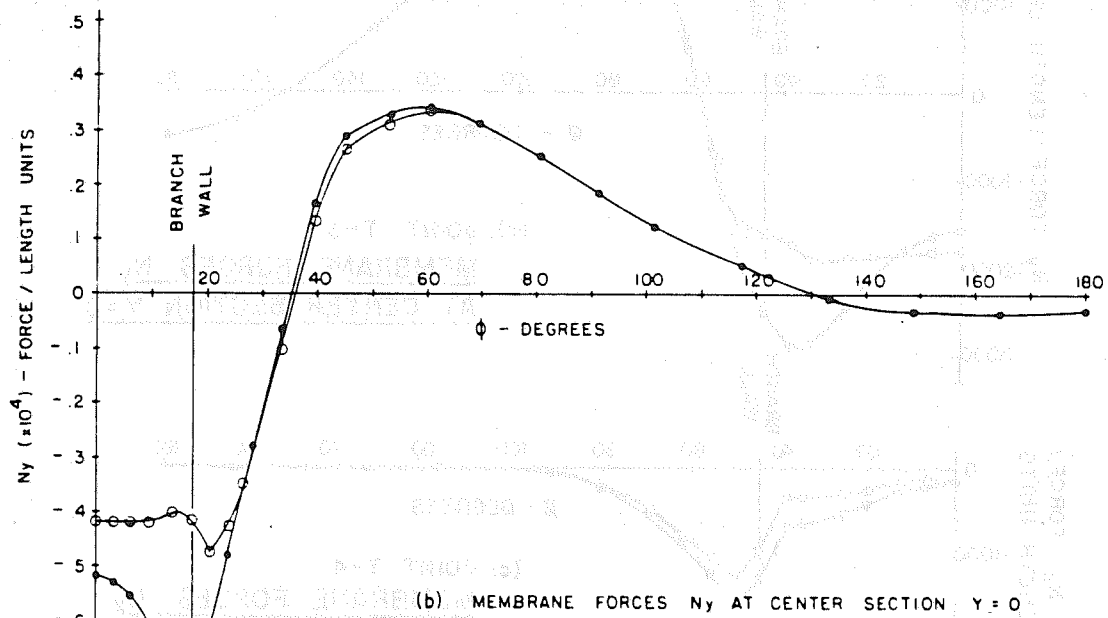
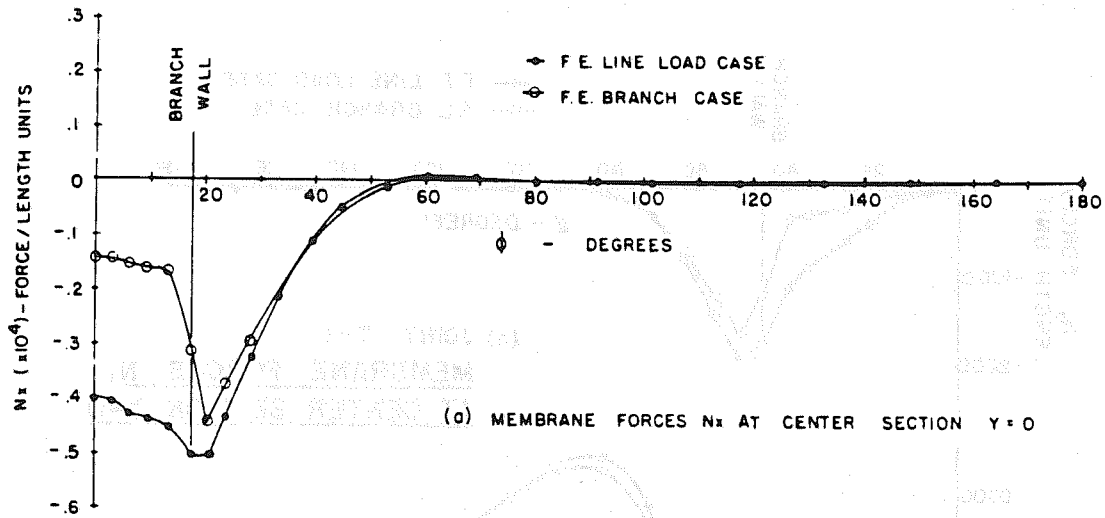


FIG. 18 LINE LOAD - BRANCH CASE
MEMBRANE FORCES, JOINT T-1

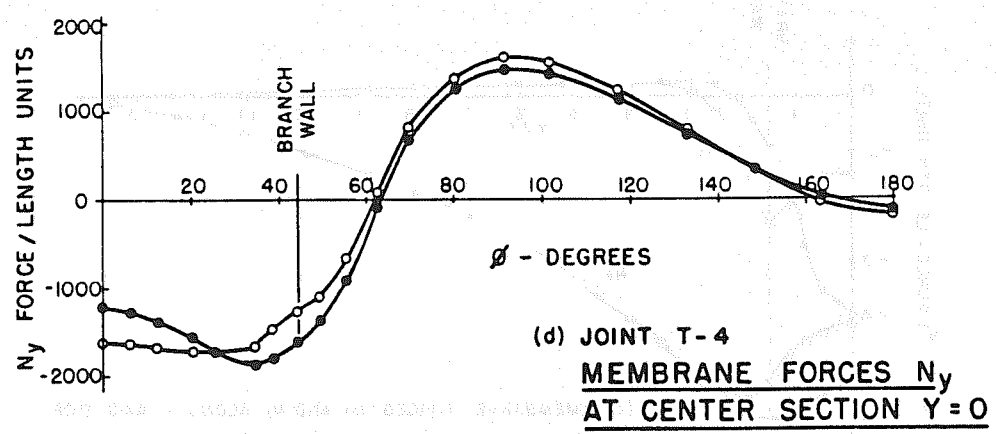
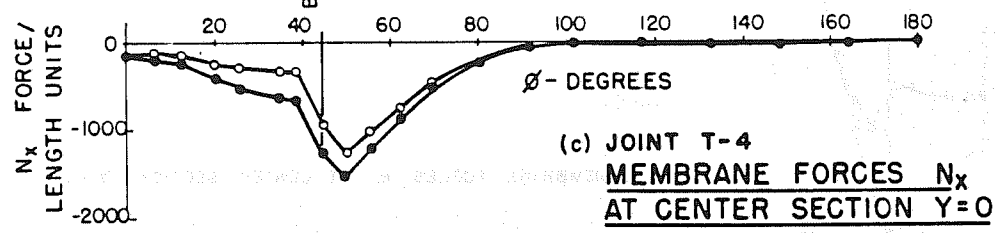
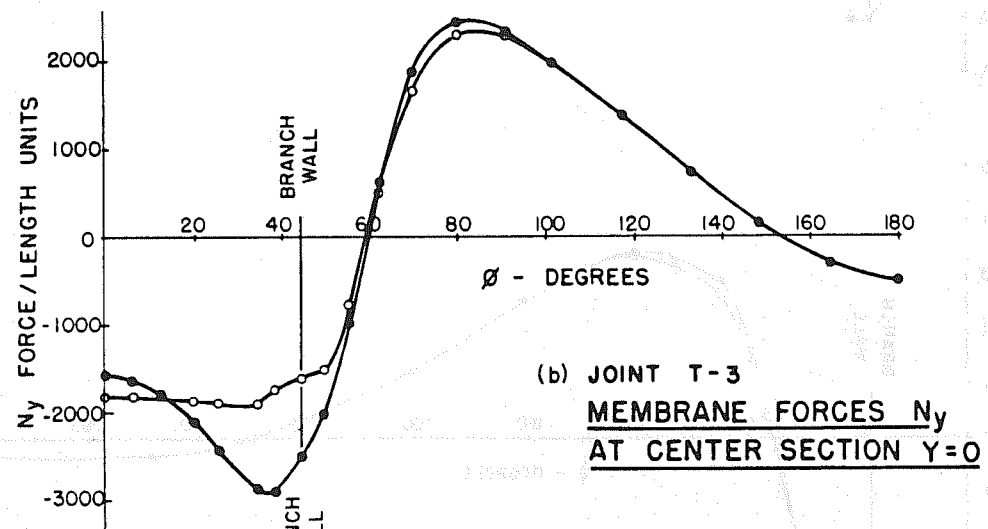
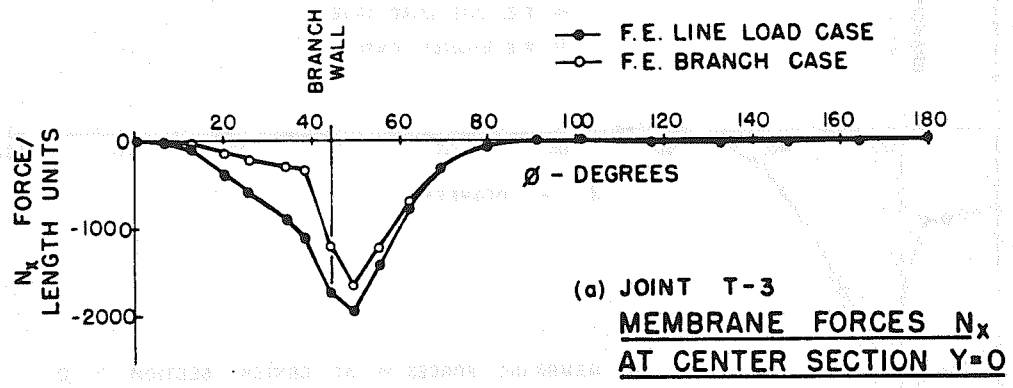


FIG. 19 LINE LOAD - BRANCH CASE
MEMBRANE FORCES, JOINTS T-3 AND T-4

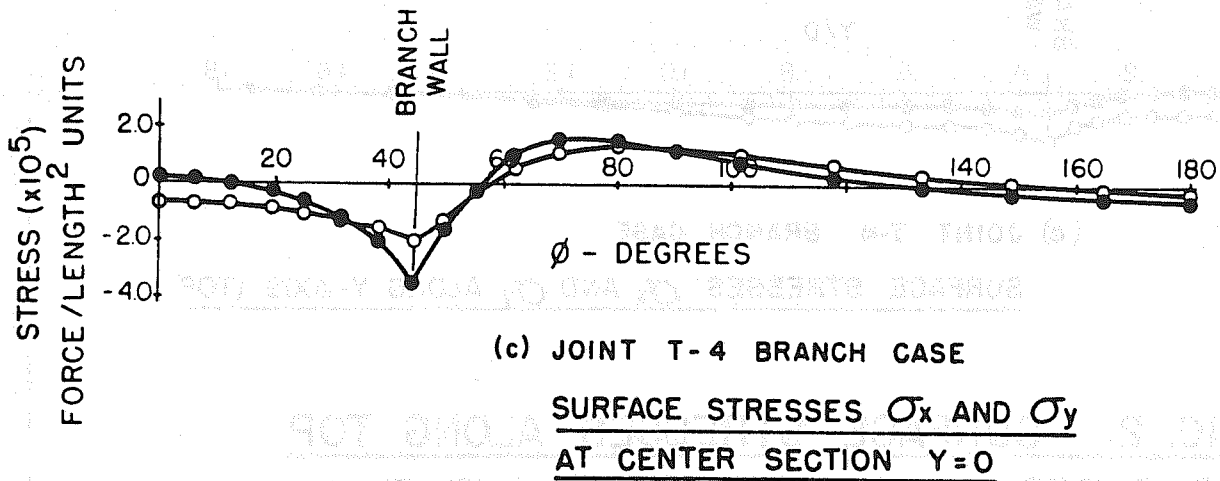
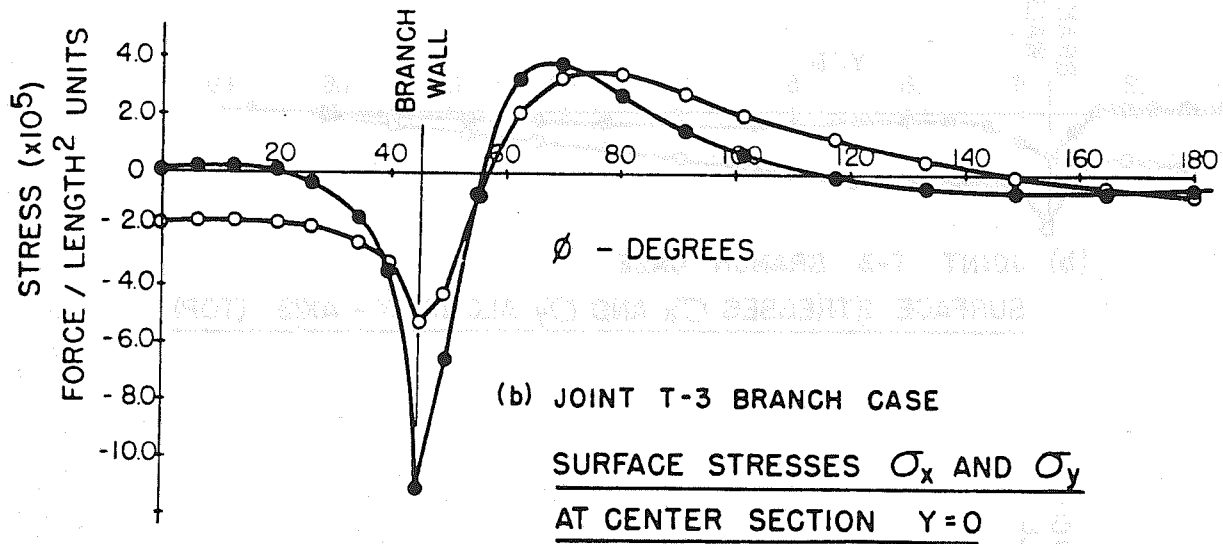
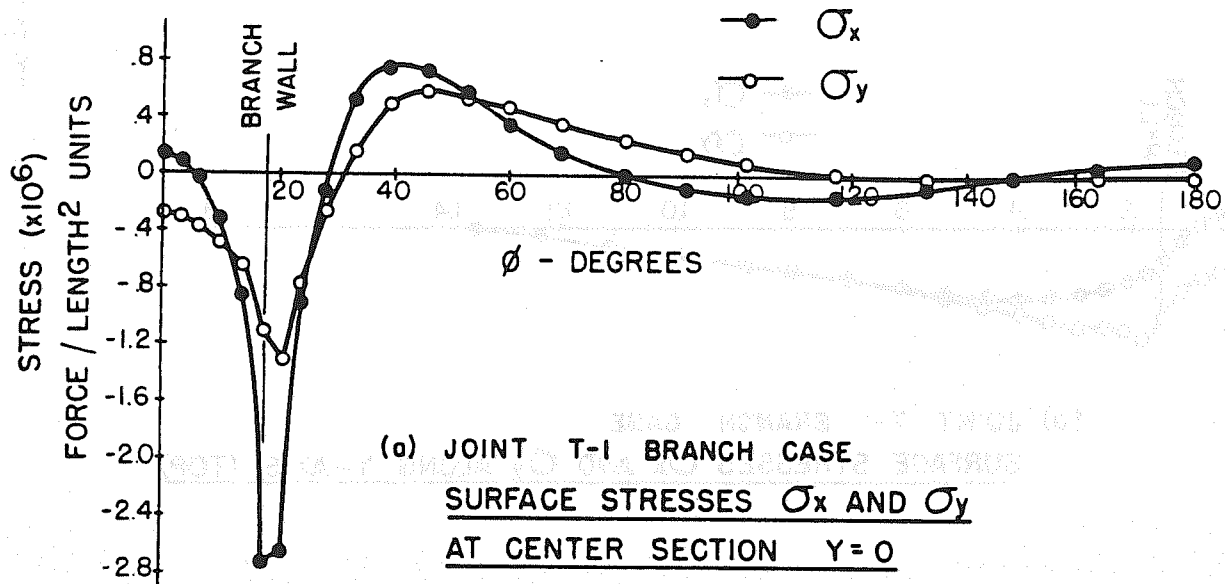


FIG. 20 SURFACE STRESSES AT CENTER SECTION, JOINTS T-1, T-3 AND T-4

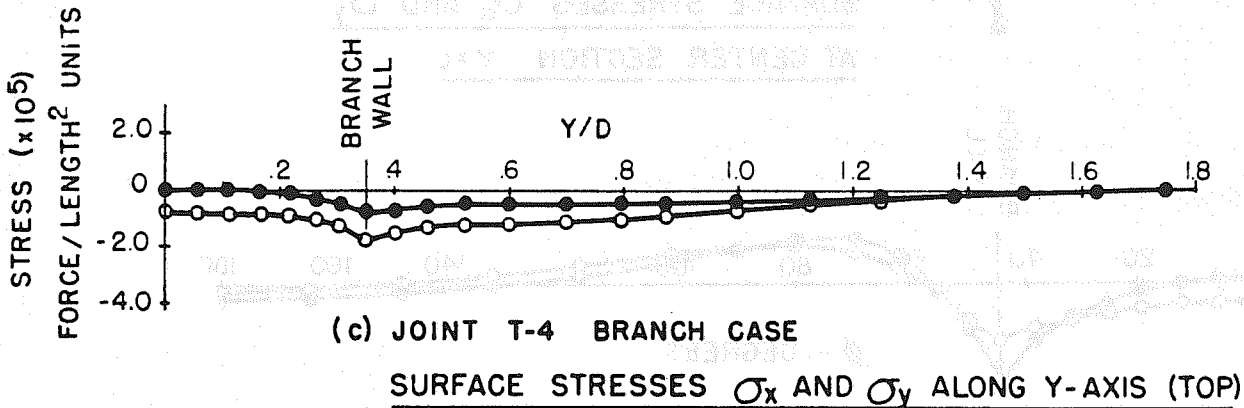
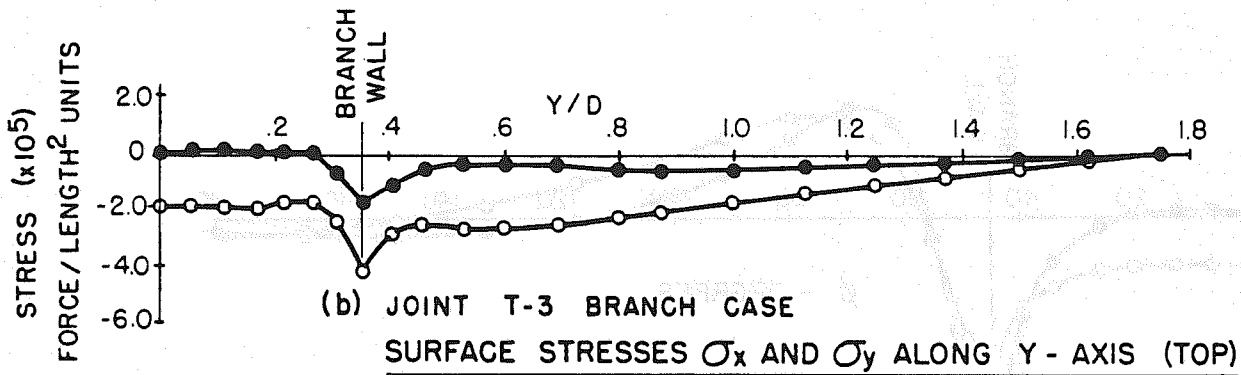
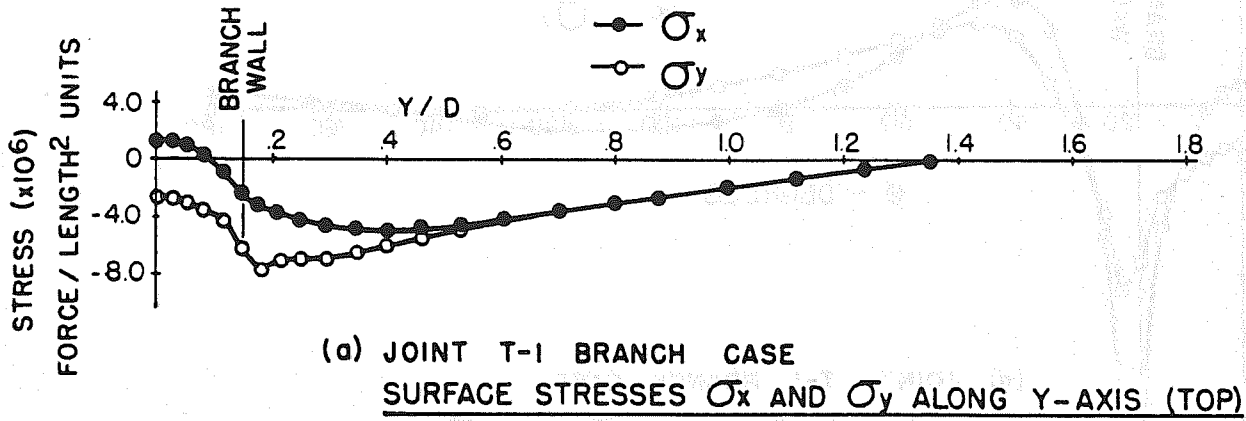


FIG. 21 SURFACE STRESSES ALONG TOP OF CHORD, JOINTS T-1, T-3 AND T-4

DIRECTION OF Y - AXIS \longrightarrow

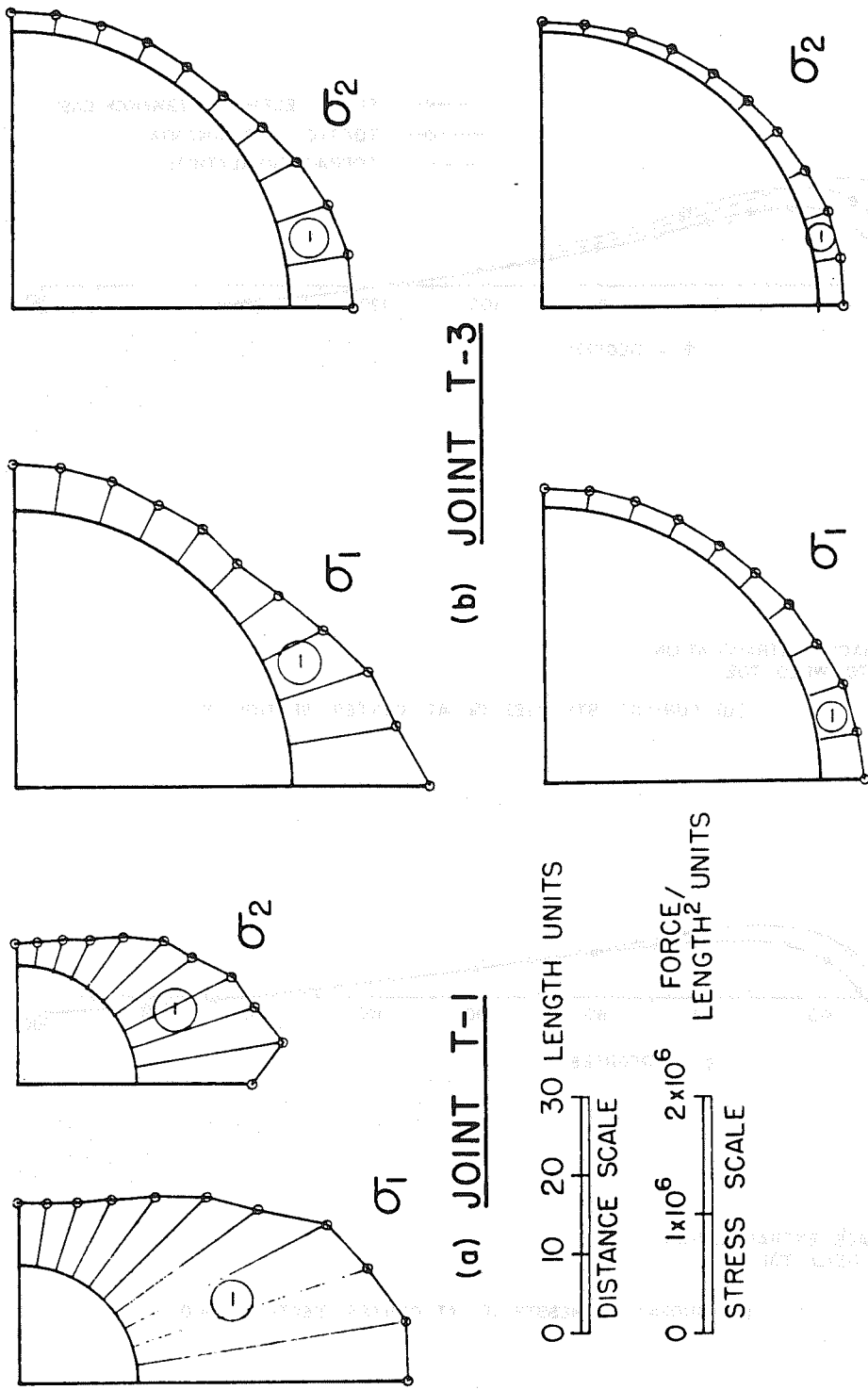


FIG. 22 PRINCIPAL STRESSES AT PIPE INTERSECTION

JOINTS T-1, T-3 AND T-4

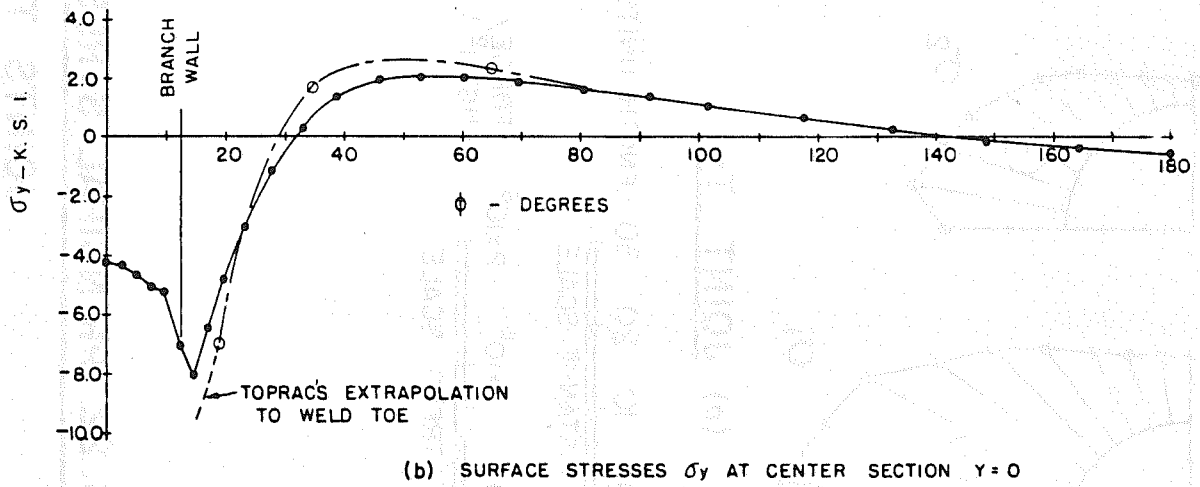
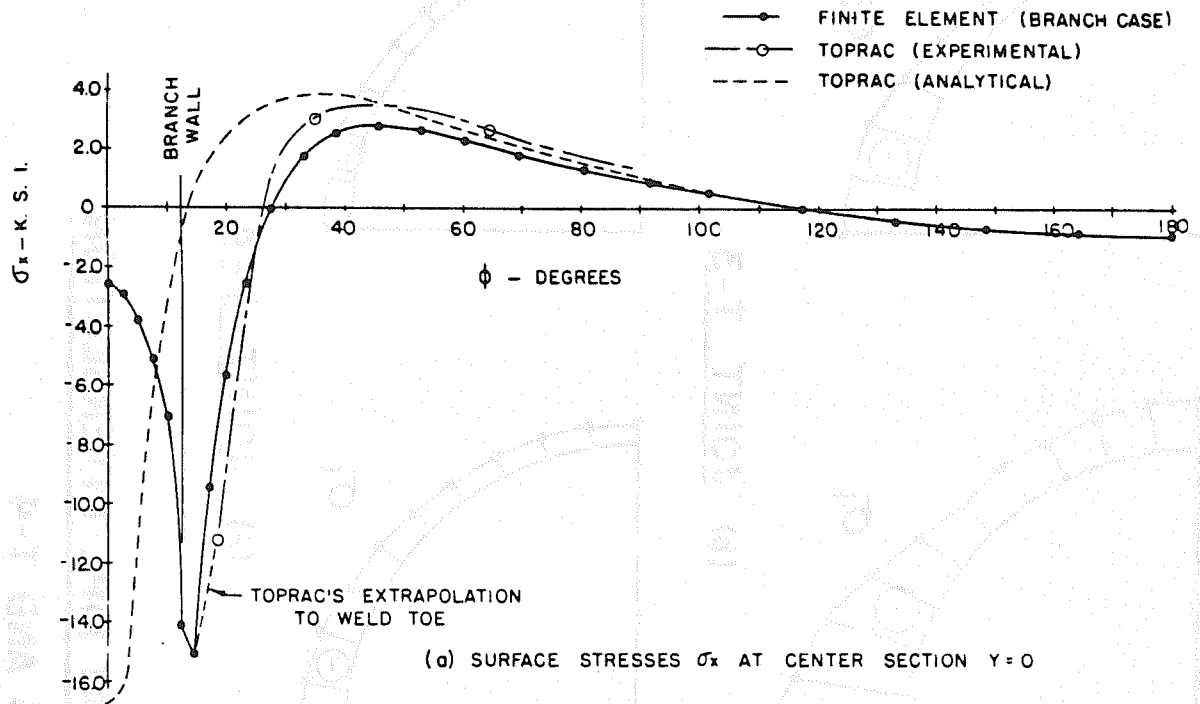
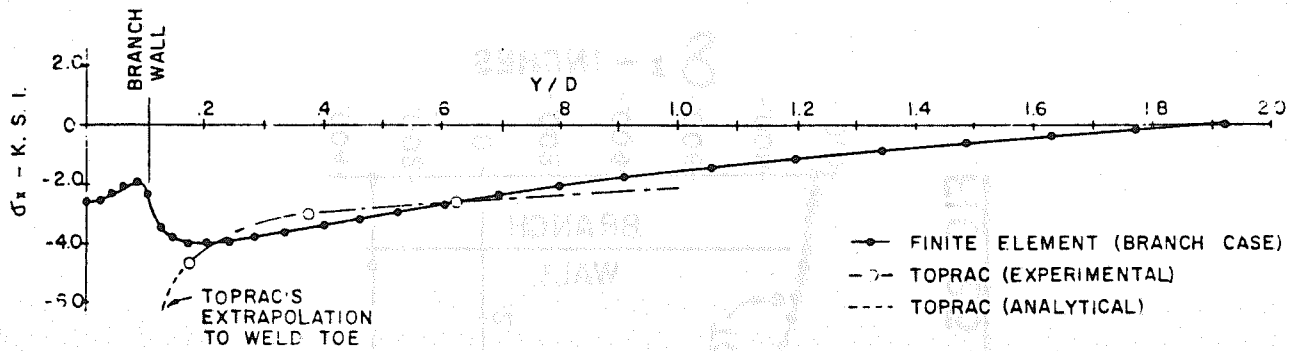
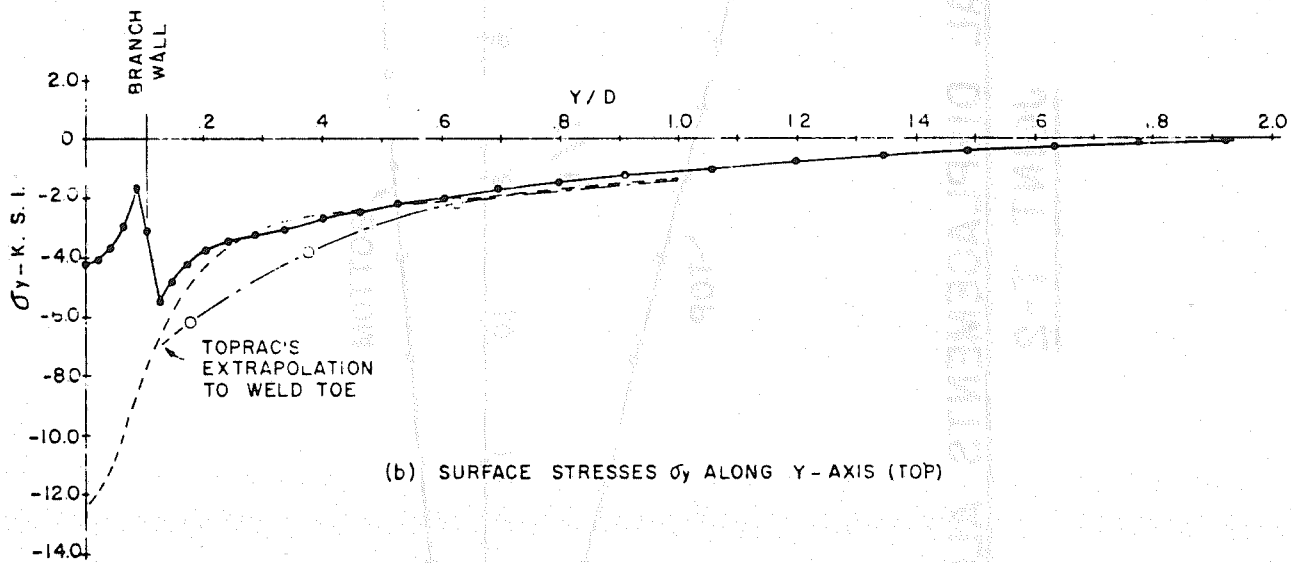


FIG. 23 SURFACE STRESSES AT CENTER SECTION, JOINT T-2



(a) SURFACE STRESSES σ_x ALONG Y-AXIS (TOP)



(b) SURFACE STRESSES σ_y ALONG Y-AXIS (TOP)

**FIG. 24 SURFACE STRESSES ALONG
Y-AXIS, JOINT T-2**

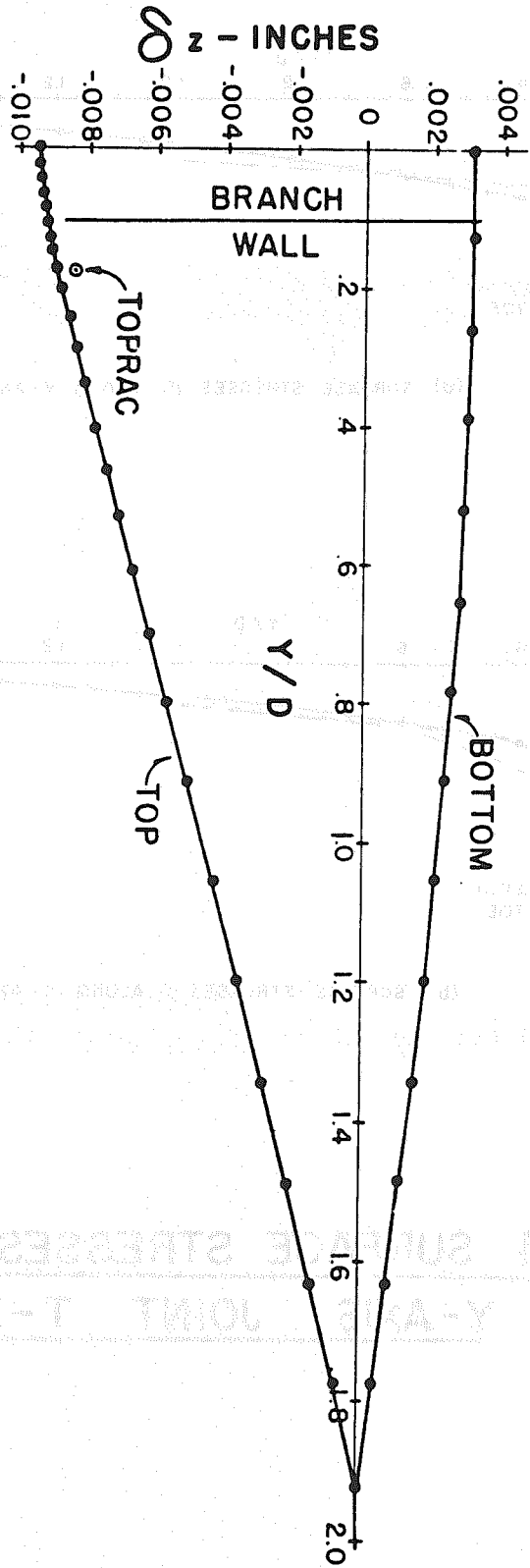


FIG. 25 VERTICAL DISPLACEMENTS ALONG Y-AXIS

JOINT T-2

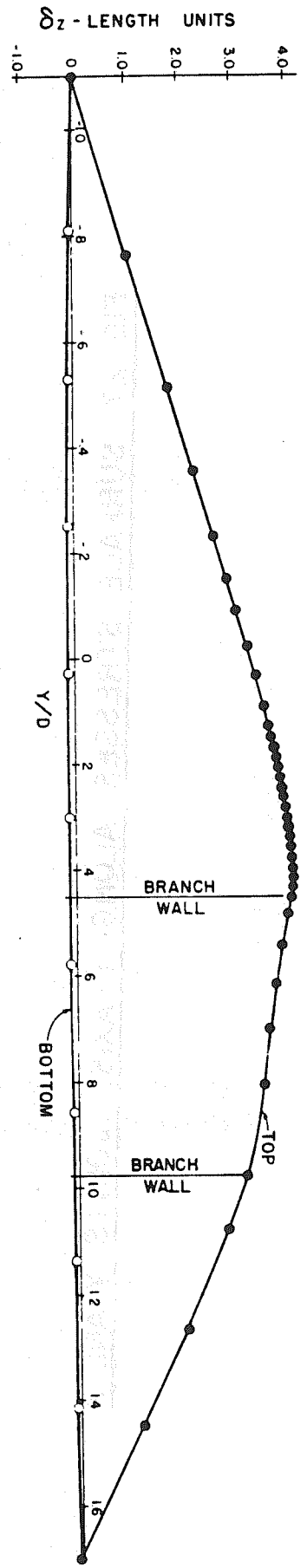
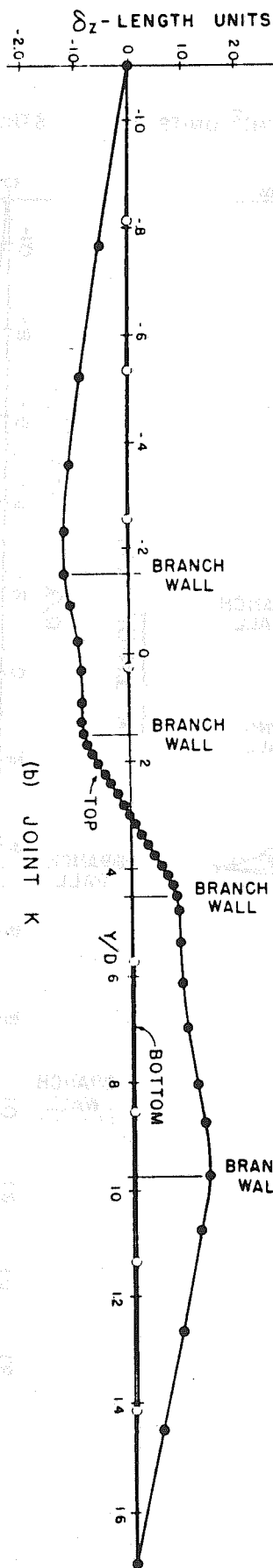
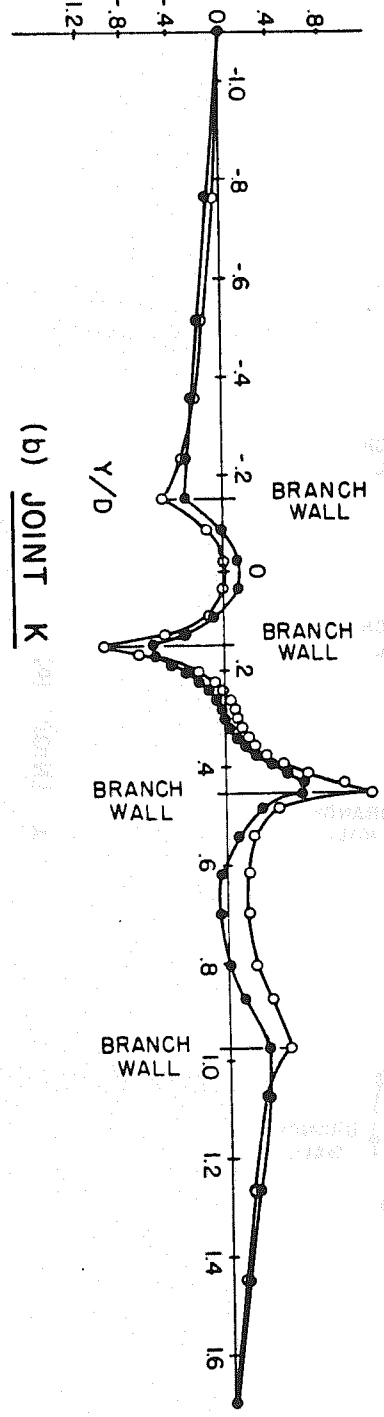


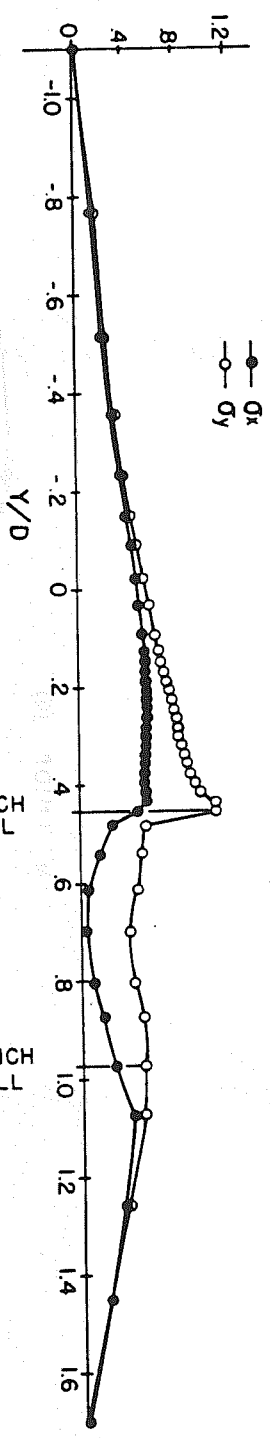
FIG. 26 VERTICAL DISPLACEMENTS ALONG Y-AXIS, JOINTS Y AND K

STRESS - FORCE / (LENGTH)² UNITS
(x 10⁶)



(b) JOINT K

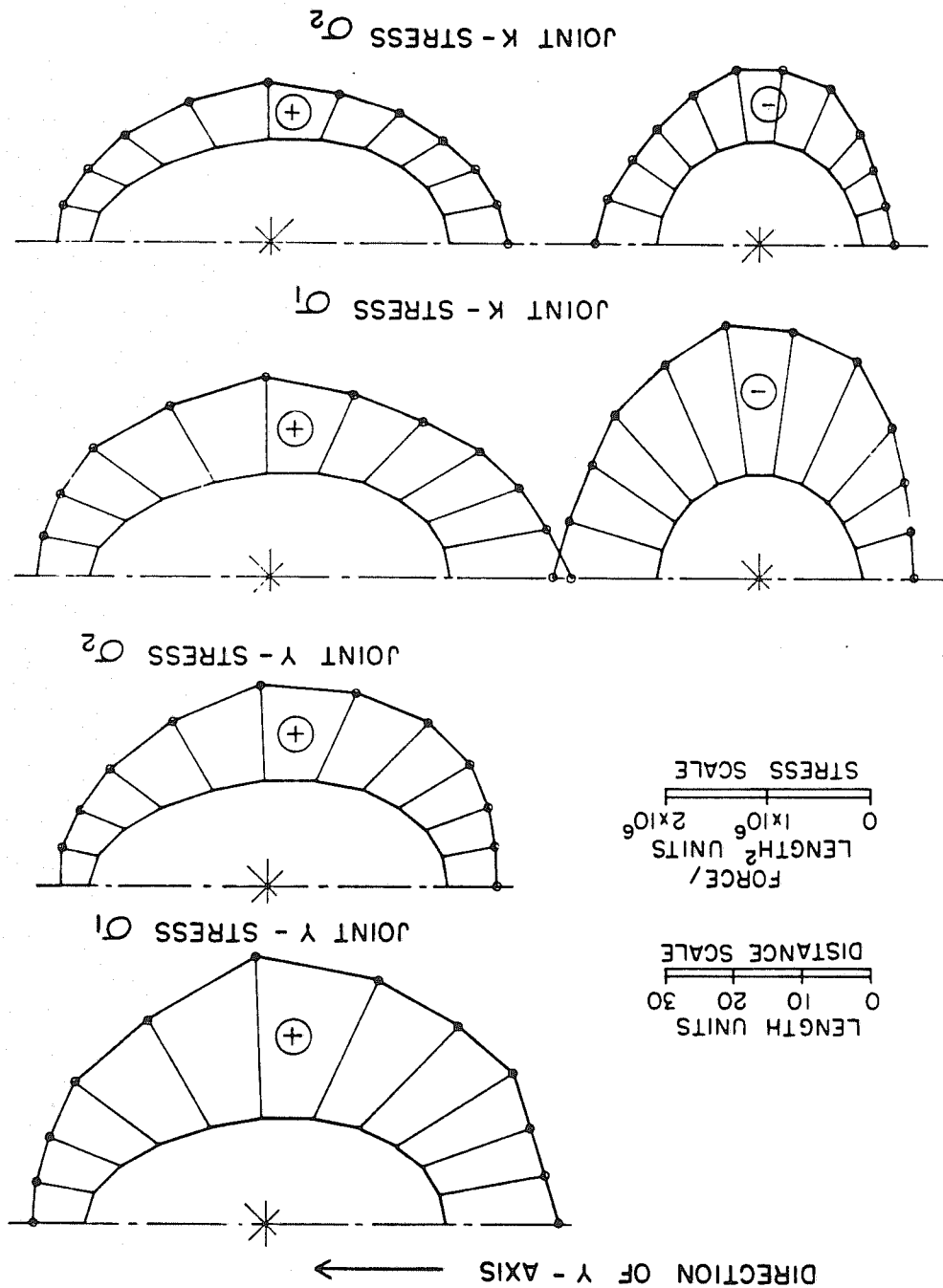
STRESS (x 10⁶)



(d) JOINT Y

FIG. 27 SURFACE STRESSES ALONG Y-AXIS, JOINTS Y AND K

FIG. 28 PRINCIPAL STRESSES AT PIPE INTERSECTION, JOINTS Y AND K



INTERSECTION POINTS A AND B
 OF THE SURFACE STRESS AT THE

FIG. 1 - STRESS

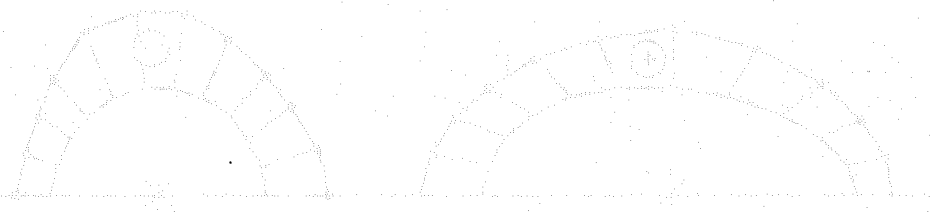


FIG. 2 - STRESS

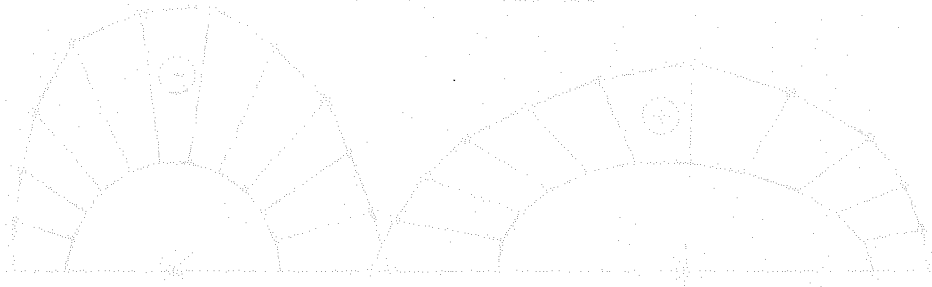
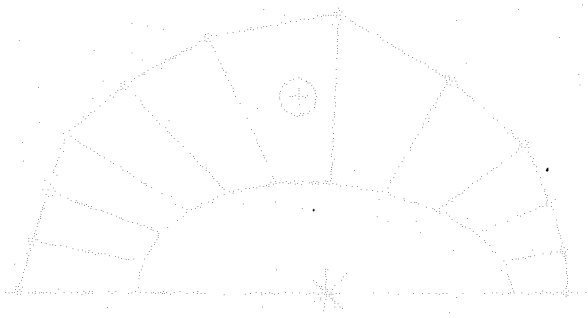


FIG. 3 - STRESS



STRESS POINT
 POINT A - CROWN
 POINT B - SPRING LINE

FIG. 4 - STRESS



STRESS POINT
 POINT A - CROWN
 POINT B - SPRING LINE

DIRECTION OF FLOW →